FLUID-CRACK INTERACTION IN HYDRAULIC FRACTURING

by

HARSHIL VORA

Presented to the Faculty of the Graduate School of

The University of Texas at Arlington in Partial Fulfillment

of the Requirements

For the Degree of

MASTER OF SCIENCE IN MECHANICAL ENGINEERING

THE UNIVERSITY OF TEXAS AT ARLINGTON

May 2015

ACKNOWLEDGEMENTS

I hereby take this excellent opportunity to acknowledge all the help, guidance and support that I have received for completion of my thesis. I would like to thank my advisor, Professor Bo Yang, for all of his help in completing this thesis. My interest in hydraulic fracturing was first piqued last fall when I stopped by Professor Yang's office. I was lucky enough to have the opportunity to learn from him throughout my graduate study. Thank you Dr. Yang for always being available and open minded, and for making the thesis-writing processes such an enjoyable experience. I could not have asked for better guidance.

I am grateful to Dr. Kent Lawrence and Dr. Hyejin Moon for serving my thesis committee and evaluating my work.

Most importantly, I would like to thank my parents, Atul Vora and Kiran Vora, for their support and blessing. I would also like to express thanks to my friends Rohan Nilawar, Yogesh Patekari and Ameya Mathakari for their help and moral support. Lastly I would like to thank all those who directly or indirectly helped me throughout my work.

April 29, 2015

ABSTRACT

FLUID - CRACK INTERACTION IN HYDRAULIC FRACTURING

Harshil Vora, MS

The University of Texas at Arlington, 2015

Supervising Professor: Bo Yang

Hydraulic fracturing has been one of the major improvements in petroleum engineering in the past few decades. Since then this process has been used progressively and over million wells have been fracked using hydraulic fracturing technology. A thorough understanding of the formation of fracture network and its propagation is essential to keep evolving the technology. In the present study, the Linear Elastic Fracture Mechanics (LEFM) approach is applied to the crack propagation to understand the fluid crack interaction in brittle rocks under hydraulic loading. The boundary element method (BEM) is used to carry out the numerical analysis. Additionally, an explicit crack representation is used to update the crack during propagation. This explicit representation is applied to a fluid-filled crack in an impermeable, elastic solid and compared to the plane-strain hydraulic fracture problem with a fluid lag. This effort provides the oil and gas industry with more knowledge and understanding of fluid crack interaction in fracking.

TABLE OF CONTENTS

LIST OF ILLUSTRATIONS

LIST OF TABLES

Chapter 1

INTRODUCTION

Energy has always been major contributor in economic wealth. Till today, a major portion of the world's energy requirement is sufficed by exploiting conventional energy reserves, which includes fossil fuels such as oil, gas and coal, found in reservoirs underneath the earth surface. Oil and gas, formed from the dead remnants of plants and animals, thousands of meters below the earth surface migrate upwards till they are trapped in rock structures shaped by folding/faulting of sedimentary layers. The trapped oil and gas found in large reservoirs is then released by drilling a long hole, vertically, into the earth with an oil rig. These energy sources are generally non-renewable and their extensive use over years has led to their depletion to a great extent. As per Energy Information Administration (EIA), in 2012, world's total primary energy consumption was 528 quadrillion btu., 1.5% increase from previous year with China and United States contributing to 20% and 18% of the total consumption respectively. The depletion of conventional energy resources and exponential hike in energy consumption has led to the oil and gas companies to explore for alternative method of energy harvesting. A promising unconventional energy resource, like shale gas, coal beds and tight sands, trapped in void spaces between impermeable rocks cannot migrate upwards to form a conventional gas reservoir. Shale gas serves as the alternative source to meet the increasing demand of energy.

Energy Information Administration (EIA) reported, till 2013, United States had 309 trillion cubic feet of natural gas reserves. There has been 2% - 4% increase in consumption of natural gas in United States every year. Texas produced 29% of America's natural gas in 2013, making it the prominent natural gas producer among the states.

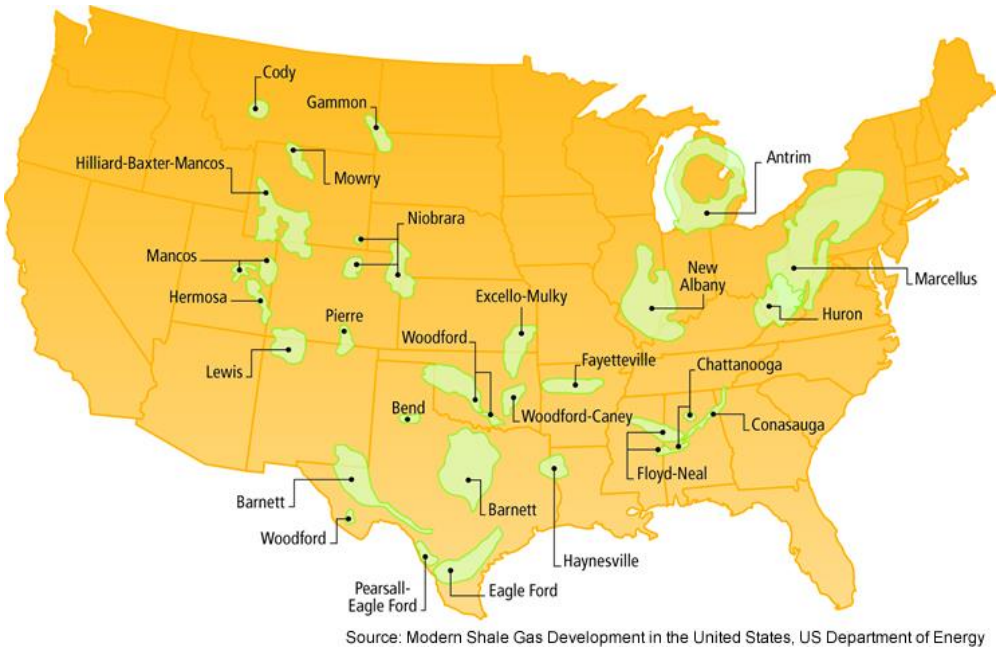

Figure 1.1 Shale gas reserves in United States. Courtesy of Baker Hughes

The concept of resource triangle was published by Master's, J.A. (1979), which says that oil and gas resources are distributed log normally in nature, just like other elements found in earth's crust. Apex of the resource triangle covers the conventional reservoirs which are normally small in size and easy to develop. As we move down the resource triangle, we find the unconventional reservoirs with

large volumes of oil or gas in place that are generally much more difficult to develop. Because of the log-normal distribution of natural resources, the volumes of oil and gas that are stored in these unconventional reservoirs are substantially higher than the volumes of oil and gas found in conventional reservoirs (Chaudhary, 2011).

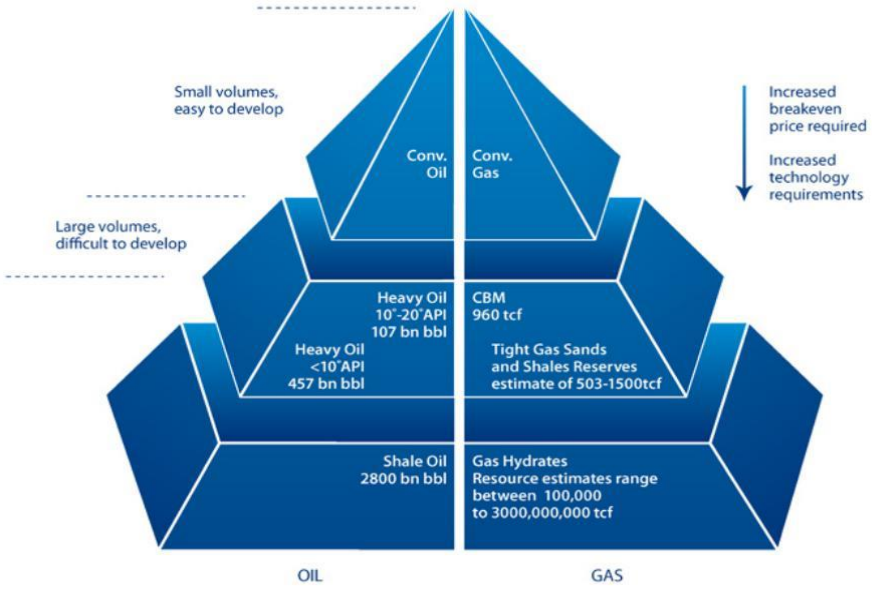

Figure 1.2 Economic and technological tradeoffs of unconventional resources, courtesy of Wood Mackenzie.

1.1 Horizontal Drilling

In recent past, to extract oil and gas trapped in large reservoirs, vertical drilling method was used. At the site location, vertical wellbore was drilled and only the area immediately at the end of the wellbore was stimulated for extraction

purpose. Once the wellbore was beyond the fresh drinking water reserve mark, the surrounding rocks were then hydraulically fractured and the trapped oil and gas was extracted.

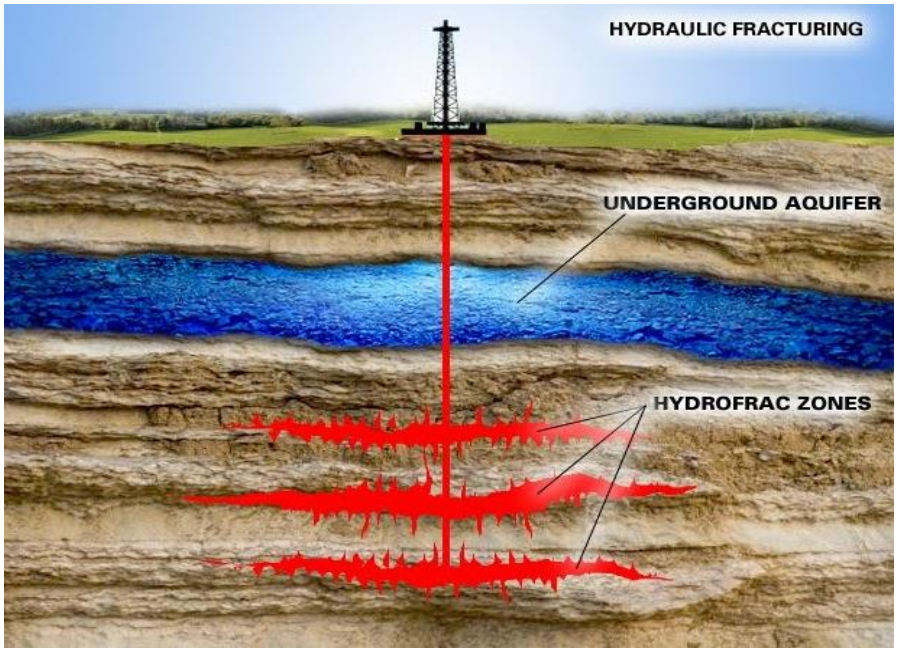

Figure 1.3 vertical hydraulic fracturing. http://stephenleahy.net/tag/hydraulic-fracturing/

Over the years energy industry has engineered the fracking process and come up with new method of stimulating oil reserves, horizontal drilling or directional drilling. In past decade, many new wells have been fracked using horizontal or directional drilling technology. S.D. Joshi (1991) published in his book “Horizontal Well Technology”, the main purpose of using this technology is to stimulate reservoir volume and thereby increase the production index.

Figure 1.4 gives the clear understanding of the depths and the extraction methods of different types of gas compared to the conventional extraction of gas.

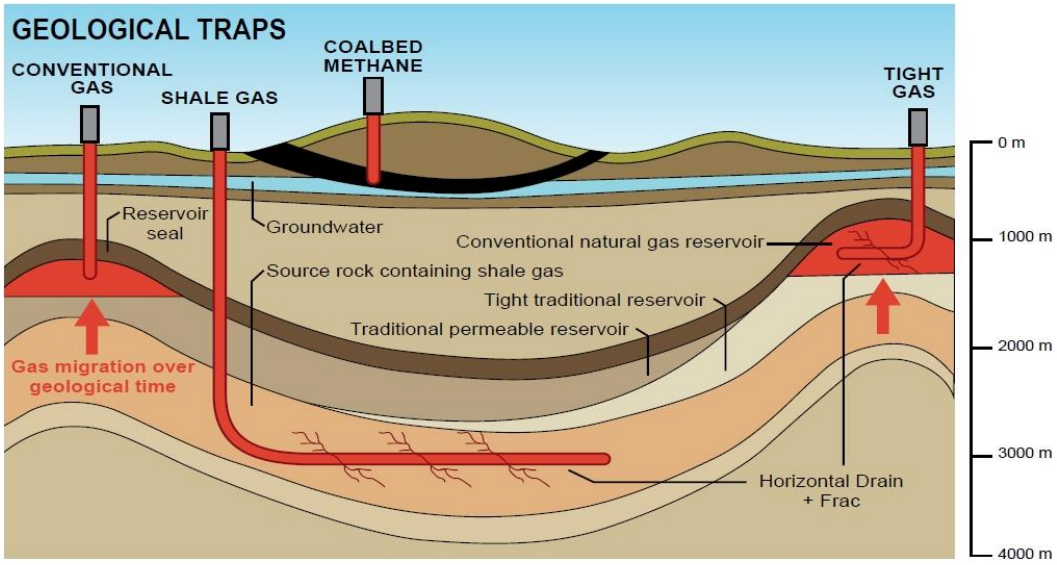

Figure 1.4 Summaries of the depth and extraction methods of different types of gas resources compared to traditional extraction of natural gas.

www.dmp.wa.gov.au/onshoregas.

Reasons of using horizontal drilling technique can be summarized as below:

1. Areas difficult to reach with vertical drilling can now be exploited.

In developed countries like United States, sometimes gas reservoir is under residential area, commercial complex, park etc. where drilling is impossible or prohibited. In such situations, oil and gas industry sets up the drilling pad site adjacent to the reservoir (bit away from the residential area or off park limits)

from where the wellbore is first drilled vertically and then horizontally to extract the trapped natural gas.

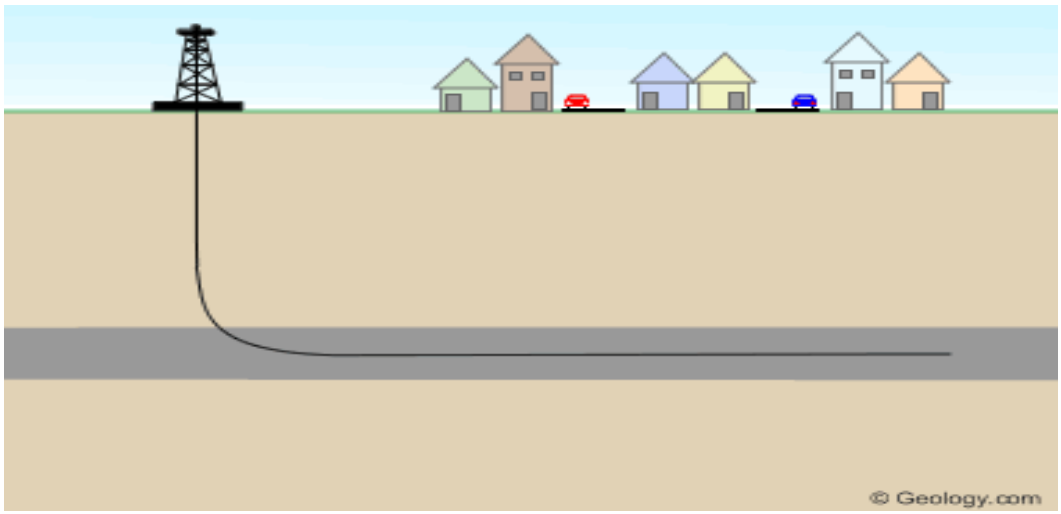

Figure 1.5 Target Area exploited using horizontal drilling.

http://geology.com/articles/horizontal-drilling/

2. Drain a large area from one single pad site.

In 2010, 22 wells were drilled on a single pad site beneath The University of Texas at Arlington campus that will drain natural gas from 1100 acres campus. The wells are expected to produce a total of 110 billion cubic feet of gas. This technique considerably reduced the footprint of natural gas development within the campus area. Figure 1-6 shows a large area being drained from a single site.

3. Improve the rate of production in a fractured reservoir.

At times, some reservoirs have the void spaces in the form of fractures. Drilling a well intersecting maximum naturally occurring fracture will cause large

amount of natural gas to flow back into the well. In Figure 1-7, Horizontal drilling when combined with hydraulic fracturing can make a well more productive where the vertical well would have produced small amount of natural gas.

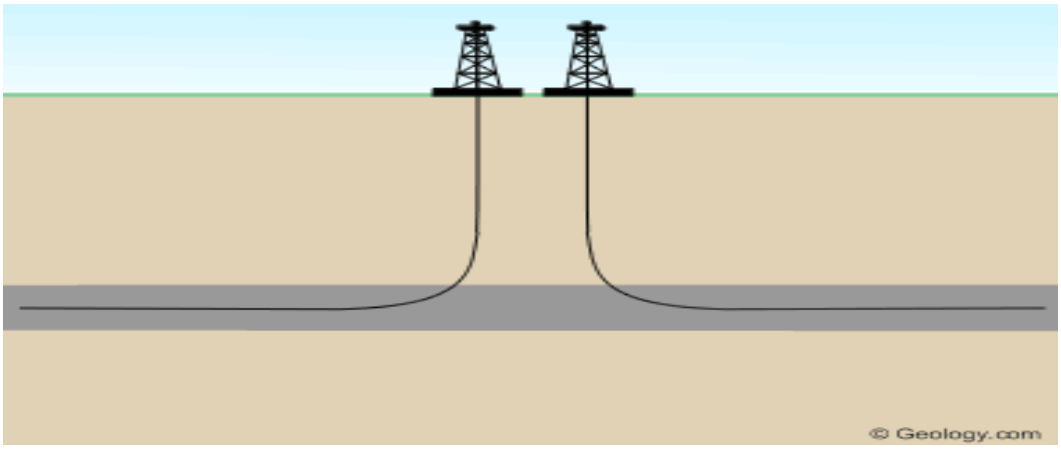

Figure 1.6 Drain a large area from one single pad site.

http://geology.com/articles/horizontal-drilling/

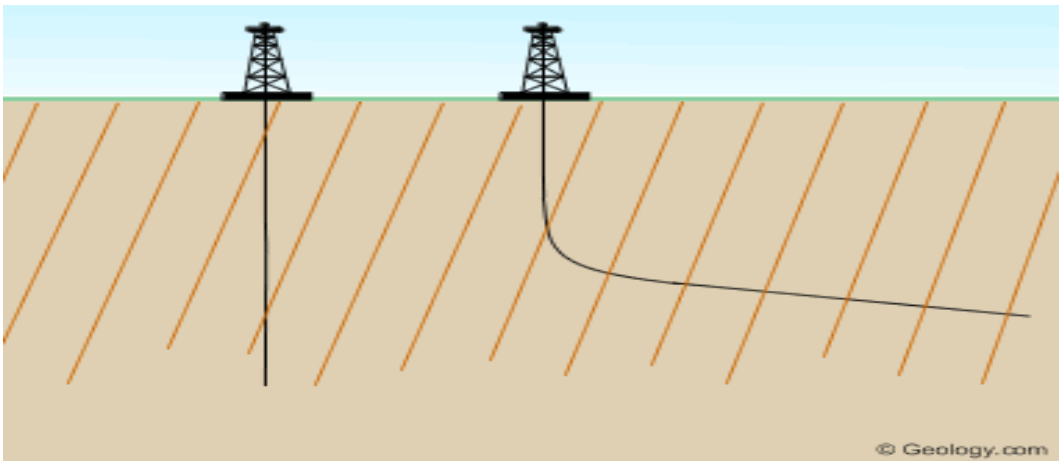

Figure 1.7 Improve the rate of production in a fractured reservoir.

http://geology.com/articles/horizontal-drilling/

When horizontal drilling is combined with hydraulic fracturing, some unconventional gas reservoirs which were unproductive when drilled vertically can become rich producers of oil or natural gas. Examples are the Marcellus Shale and Barnett Shale (L Helms - DMR newsletter, 2008).

1.2 Hydraulic Fracturing

Hydraulic fracturing has been one of the major improvements in petroleum engineering in the past few decades. This technique of stimulating the gas rich reservoir was first introduced to the industry in a paper by J. B. Clark of the Stanolind Oil and Gas Company (1949). Since then this process has been used progressively and over million wells have been fracked using hydraulic fracturing (Hubbert and Willis- Mechanics of Hydraulic Fracturing- 1972). However the first hydraulic fracturing process was used in 1947 on a gas well operated by Pan American Petroleum Corp. in the Hugoton field (Gidley, J.L., Holditch, S.A., Nierode, et al. 1989). Fracturing earth's crust is preferred for many reasons, including enhancing oil and gas production, water well production, and harvesting geothermal energy (B.J. Carter, 2000).

Hydraulic Fracturing is the process of pumping highly pressurized fracturing fluid into a wellbore at an injection rate which is too high for the perforation to accept without breaking. As the resistance to the fluid increases, pressure inside the wellbore exceeds the breakdown pressure to open the perforation. Once the perforation opens, the pressurized injected fluid enters the

opening and initiates the fracturing of rocks. Depending on the high flow rates and pressure, these fractures can extend from few meters to hundreds of meters.

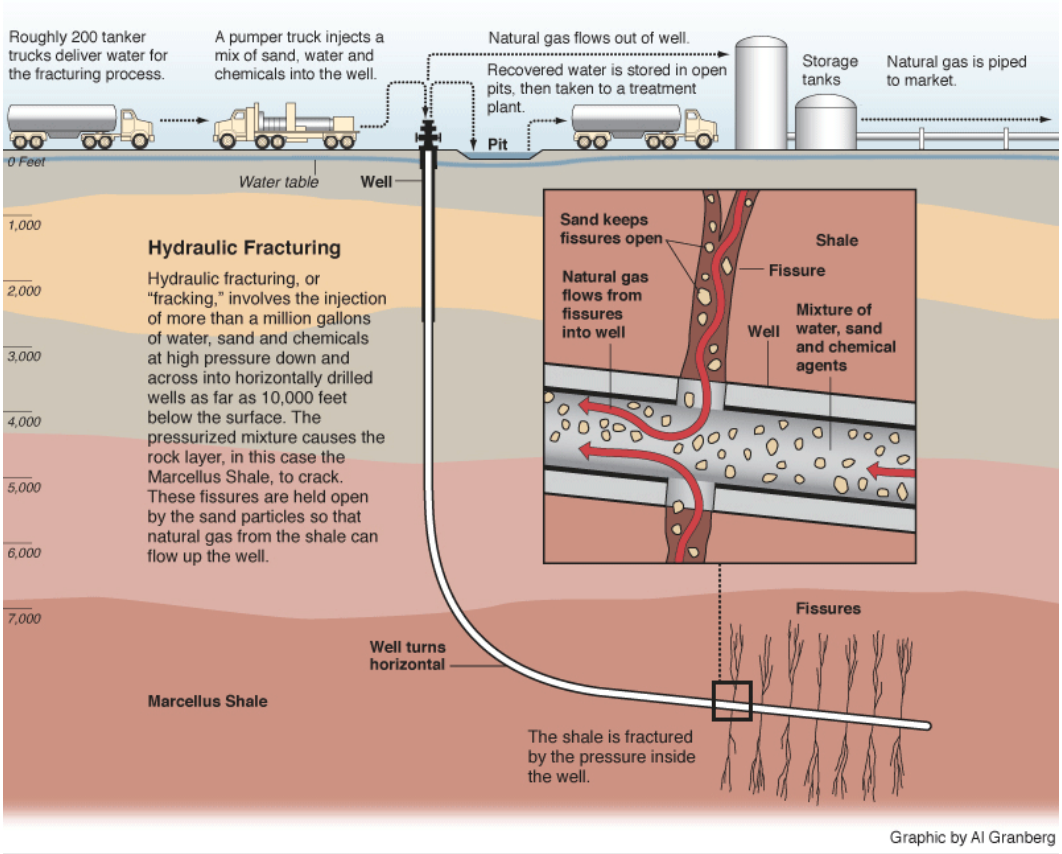

Figure1.8 Hydraulic fracturing processes in detail graphic by Al Granberg

Fractures always propagate along the path of least resistance. In 3D fracture will try to avoid the direction of maximum stress and will create width in the direction which requires least force i.e. is the direction perpendicular to the plane of least principal stress and parallel to the greatest principal stress. Fracture

propagation and its orientation depend on various factors such as stress field, material properties and fluid flow pressure.

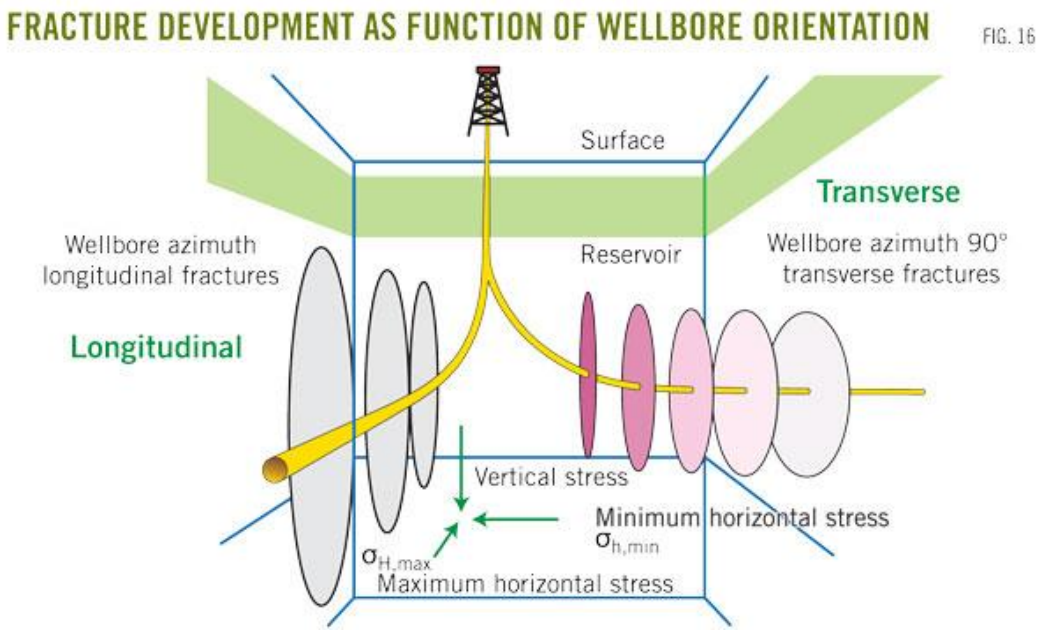

Figure 1.9 Fracture developments as function of wellbore orientation.

http://www.ogj.com/

Hydraulic fracturing is mainly divided into 2 stages.

1. Pad Stage: It consists of pressurizing approximately 100,000 gallons of water without proppant material and filling the entire wellbore with water. This process opens the crack and allows the fluid to flow inside the fracture and allow placement of proppant material. Once the fracture is wide open for the proppant material to flow inside the crack, pressurized water is flushed out during the cleanup process.

2. Slurry stage: In this stage proppant material consisting mainly of 99% sand particles and 1% chemicals, acting as catalyst facilitate fracturing process, is pressurized and directed into the wellbore to keep the fracture open to allow the natural gas to flow freely from fracture to wellbore and is then directed out. As the granular proppant extends a considerable distance into the fracture from the borehole into the crack, releasing the pressure. The sides of the fracture to compress onto the proppant, creating a high-permeability corridor to allow natural gas to flow back to the well and to the surface (Charles Fairhurst, Effective and sustainable hydraulic fracturing).

1.3 Objective of the study

Despite of having a few disadvantages, hydraulic fracturing has gained popularity over years. Fracking has always been related to the cause for damaging environment. A recent example of drinking water reserve being polluted by extraction of shale gas in Pennsylvania had oil and gas companies reach out to researchers for making hydraulic fracturing a more controlled operation. Understanding the complex structure of cracks formed during fracturing and its propagation is crucial for oil and gas companies. Researchers have studied many models to interpret the, propagation of fluid driven crack with fluid lag (Dmitry I. Garagash, 2005), equilibrium of pressurized fluid in the wellbore crack (Dmitry I. Garagash, Erfan Sarvaramini, 2011), but the interaction between pressurized fluid and crack surface has not been studied in great detail. A paper published by D.

Garagash and E. Detournay, 1996) shows the dependence of breakdown pressure on the pressurization rate. Breakdown, in context to hydraulic fracturing, occurs when the stress intensity factor (SIF) overcomes the rock toughness. As published in the book, 'Effective and Sustainable Hydraulic Fracturing', an attempt was made by Azadeh Riahi and Branko Damjanac, on the numerical modelling of fluid injection into the fractured rock and the interaction between hydraulic fracture and the discrete fracture network. The analysis carried out by them was based on distinct-element modelling approach without considering fluid lag, rendering the results to be less accurate.

Figure1.10 View of fractured rock. Courtesy of Baker Hughes.

The emphasis of the present study is on the interaction between the pressurized fluid injected into the fracture channel and the crack surface. My contribution will be to model the propagation of the fluid driven crack and elucidate the mechanics behind the fluid-crack interaction.

Chapter 2

LITERATURE REVIEW

2.1 Fluid mechanics formulation

Single phase fluid flow through fractured wall is the most basic problem in rock hydrology (R.W. Zimmerman and Yeo, 2000). The study forms the foundation for understanding multiphase flow, fluid flow through fracture networks etc. A lot of research has been carried out on this topic, still far from being understood completely. Fundamentally, flow through fractured rock is governed by Navier Stokes (N-S) equations.

$$\underbrace{\rho(u\,\nabla)u}_{\text{Advective}} = \underbrace{-\nabla P}_{\text{Pressure}} + \underbrace{\mu\nabla^2 u}_{\text{Viscous}} \qquad (1)$$

Acceleration gradient forces

where ρ is the density, u is the velocity vector, μ is the viscosity, and ∇P is the pressure gradient along the length of the crack. Mathematically, it is desired to understand of the situations under which Navier-Stokes equations can be used and when it can be replaced by Stokes equation or lubrication equation.

Unfortunately, the full Navier-Stokes equations are too challenging to solve, either analytically or numerically, for real, fluid flowing through fractured cracks. This is also true for idealized fracture geometries such as a fracture bounded by linear drop in the aperture height. Therefore, various approximations are usually made that reduce the N-S equations to a more tractable form. The first

level of simplification is to discard the acceleration terms in the Navier-Stokes equations; we usually consider fluid flowing in one direction. The aperture of the fracture varies in only one direction i.e. in *x* direction, taken as the direction of fluid flow, direction perpendicular to the plane of fracture propagation *y*. The Navier-Stokes equations must always be supplemented by the equation for conservation of mass, which for an incompressible fluid, $\rho = 0$, takes the form:

$$\nabla . \mathrm{u} = 0 \tag{2}$$

This yields the steady-state Stokes equations, a coupled set of three linear partial differential equations:

$$\nabla P = \mu \nabla^2 u \tag{3}$$

When the flow is governed by Stokes equation, it implies a linear relation between pressure gradient and flow rate i.e. Cubic Law

2.2 Flow between parallel plates

The initial point for all discussions of the fracture flow problem is the special case of a fracture bounded by smooth, parallel plates that are separated by a distance h.

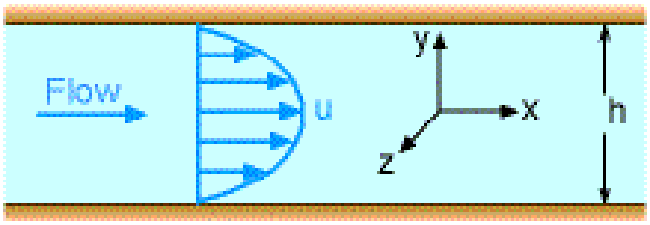

Figure 2.1 Fluid flow between parallel plates. www.eng.usf.edu

This is, in fact, the only fracture geometry for which the N-S equations can be solved exactly. The simplification of the N-S equations in this case arises from the fact that the velocity vector points in the x-direction, but it varies only in the y-direction. Hence, the velocity and the velocity gradient are orthogonal to each other, and the nonlinear term on the left-hand side of Equation (1) vanishes identically. Fluid flows between the parallel plates from inlet to outlet as marked by arrow. The common boundary condition used is constant static pressure at inlet and outlet. The fracture walls are impermeable and rigid (no slip boundary condition). The velocity vector for flow between smooth, parallel plates is given by (R.W. Zimmerman and Yeo, 2000) integrating equation (3) twice as:

$$Ux(y) = -\frac{1}{2\mu}\frac{dP}{dx}\left[y^2 - \left(\frac{h}{2}\right)^2\right] \tag{4}$$

The velocity profile, when integrated across the fracture opening, gives the total flow rate in the form:

$$Qx = \int_{-h/2}^{h/2} Ux\, dy \tag{5}$$

$$= -\int_{-\frac{h}{2}}^{\frac{h}{2}} \frac{1}{2\mu}\frac{dP}{dx}\left[y^2 - \left(\frac{h}{2}\right)^2\right] dy \tag{6}$$

$$Qx = -\frac{h^3}{12\mu}\frac{dP}{dx} \tag{7}$$

Equation 7 gives the total flow rate for the flow between parallel plates.

2.3 Darcy's Law

Darcy's Law is described as the velocity of flow of a liquid through a porous medium due to difference in pressure is proportional to the pressure gradient in the direction of flow. Although Darcy's law is used extensively to describe the flow of fluids through permeable medium, the most common is one dimensional fluid flow with constant viscosity.

$$q = -\frac{kA}{\mu}\frac{\partial P}{\partial x} \tag{8}$$

Where q is the total discharge, k is the intrinsic permeability of the medium, A is the cross sectional area, μ is the viscosity and $\frac{\partial P}{\partial x}$ is the total pressure drop across the fracture length in x direction. From equation (7) and (8), the permeability of the fracture can be identified as:

$$k = \frac{h^2}{12} \tag{9}$$

Considering unit width 'w' the cross sectional area A is given by 'wh'. Transmissivity is describes as the product of cross sectional area and permeability and is equal to:

$$T = kA = \frac{wh^3}{12} \tag{10}$$

From equation (10), well known cubic law states the dependence of T on h^3.

Despite exact solutions for fluid flow between parallel plates, validating it for real life applications needs to be studied. In actual scenario the fractures are not bounded by smooth parallel surfaces. However, natural fractures are more

likely to be rough walled, lowering total flow. In this case, the equivalent aperture through which fluids can flow, called the hydraulic aperture, is smaller than the actual opening displacement of the fracture (Christian Klimczak, 2009).

The pursuit of correlating hydraulic apertures to the pressure applied by the fluid on the fracture surface has been met with limited success. Different approaches have attempted to find a typical hydraulic aperture by introducing an empirical relation between crack and fluid propagation based on fluid–crack interaction experiments. (Christian Klimczak, 2009).

As mentioned in equation (10), transmissivity is proportional to h^3, fluid flow in a rough walled, variable-aperture, fracture under hydraulic loading conditions will tend to follow paths of least resistance, which is, the path of largest aperture (S. Sarkar, M. Toksoz and D. R. Burns). Hence constant variable 'h' in equation (10), when replace by equivalent nonlinear hydraulic aperture h_{eq} would yield correct velocity profile and flow rate. Therefore, a more generalized form of cubic law should include the h_{eq} term and can be expressed as:

$$T = kA = \frac{w{h_{eq}}^3}{12} \tag{11}$$

Equation (11) can be applied to any fracture geometry with h_{eq} being a function of the pressure applied by the fluid on the fracture walls.

2.4 Fracture mechanics representation

There are two alternatives approach to fracture analysis: the energy rate approach and the stress intensity approach. The stress intensity approach has been applied in this study.

2.4.1 The stress intensity approach

Consider a planar, linear elastic traction-free sharp crack tip under far-field loading expressed as

$$\sigma ij = (\frac{k}{\sqrt{r}}) f_{ij}(\theta) + \sum_{m=0}^{\infty} A_m r^{\frac{m}{2}} g_{ij}^{m}(\theta) \quad (12)$$

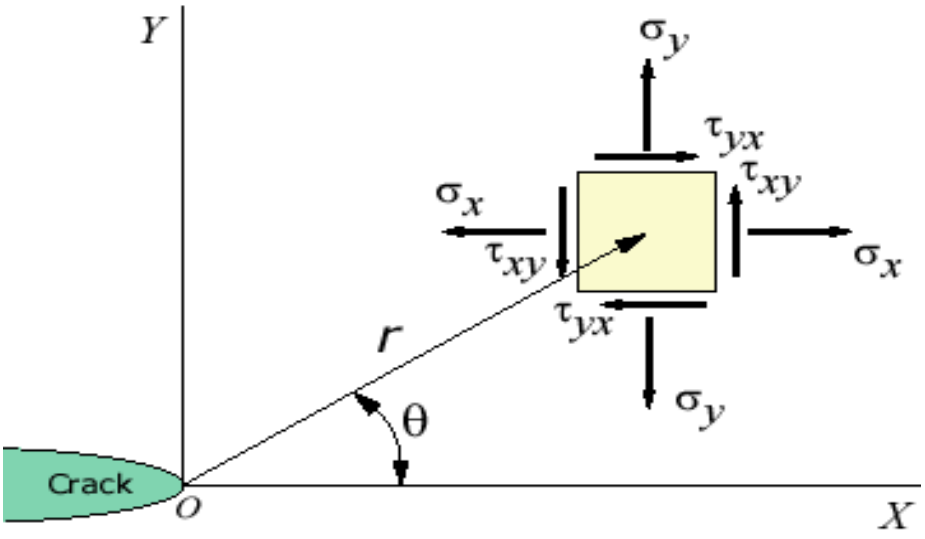

Figure 2.2 Stress field at crack tip. www.efunda.com

where, σij is the stress tensor, r and θ are defined as shown in figure 2.2. k is the constant and depend on the loading conditions and f_{ij} is the dimensionless

function of θ. The solution for any given geometry is proportional to $\frac{1}{\sqrt{r}}$. Hence at crack tip, where *r* tends to 0, the solution approaches infinity.

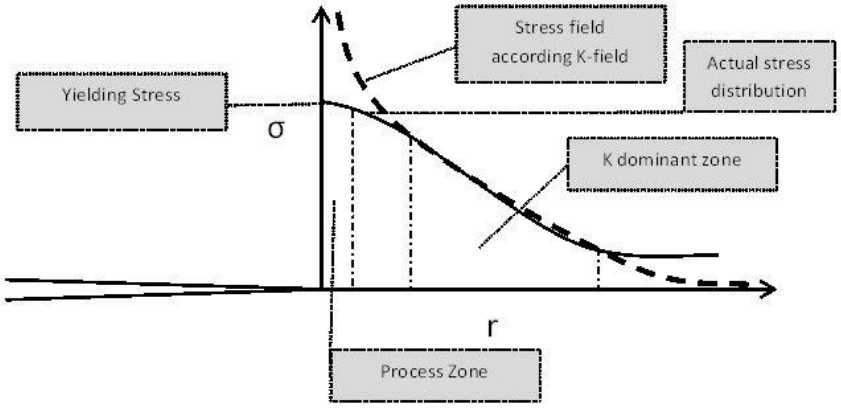

Figure 2.3 Stress intensity factor dominant zone. www.intechopen.com

From figure 2.3 it can be summarized that the amplitude of the crack tip singularity is well-defined by the stress intensity factor. That is, stress near the crack tip is directly proportional to *K*. Also the crack tip conditions can be completely defined by the stress intensity factor. Hence calculating the stress intensity factor turns out to be most important parameter in fracture mechanics.

2.4.2 Stress intensity factor

Under each loading condition a singularity of $\frac{1}{\sqrt{r}}$ is produced at crack tip. It is convenient to replace *k* with the stress intensity factor term, represented as *K*, where$K = k\sqrt{2\pi}$. The stress intensity factor is often written with fracture displacement modes as subscript; i.e. K_I, K_{II}, K_{III} and the stress fields around the crack tip can be expressed as,

$$\lim_{r\to 0} \sigma_{ij}{}^{I} = \frac{K_I}{\sqrt{2\pi r}} f_{ij}{}^{I}(\theta) \quad (13.a)$$

$$\lim_{r\to 0} \sigma_{ij}{}^{II} = \frac{K_{II}}{\sqrt{2\pi r}} f_{ij}{}^{II}(\theta) \quad (13.b)$$

$$\lim_{r\to 0} \sigma_{ij}{}^{III} = \frac{K_{III}}{\sqrt{2\pi r}} f_{ij}{}^{III}(\theta) \quad (13.c)$$

In fracture mechanics, fractures are classified into three displacement modes, as shown in figure 2.3; i.e. opening, sliding and tearing modes (Christian Klimczak, 2009).

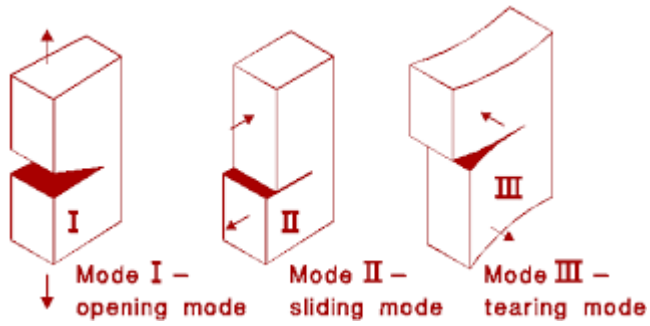

Figure 2.4 Fracture displacement modes. http://www.fgg.uni-lj.si/

This study considers an edge crack. Under ideal loading condition, the stress intensity factor for the edge crack is given by,

$$K_I = 1.12\sigma\sqrt{\pi a} \quad (14)$$

where *a*, is the length of the crack and σ is the remote stress.

It is understood that the material fails locally when the stress intensity factor reaches a critical stress intensity factor K_{IC}. So failure occurs when $K_I \geq K_{IC}$. It can be said that K_I is the driving force and K_{IC} is the material resistance. In case of fracture mechanics the fracture starts propagating once $K_I > K_{IC}$.

2.5 Mathematical Model

Fracture mechanics in connection with fluid mechanics provides the tools necessary to correlate pressure with fracture propagation properties. This involves the crack growth in elastic rock subjected to hydraulic pressure, far field stresses fracture opening, fluid flow within the fracture, fluid migration into the rock mass, etc. (F. Rummel, J. Hansen, 1989).

Consider a two dimensional hydraulic fracture under plain strain condition in an isotropic, homogenous and linearly elastic medium characterized by its Young's modulus E, Poisson's ratio ν and stress intensity factor K_{IC}. The model shown in figure 2.5 is used to study the crack propagation under zero lag condition and then the study is extended to non-zero fluid lag situation.

An incompressible fluid having pressure P_f and viscosity μ is injected into the fracture, having crack length l_f and at the constant rate q_0 to drive the fracture. As fluid pressure and viscosity are the two controlling parameters to crack propagation, pressure rise inside the fracture causes it to propagate symmetrically along the direction parallel to greatest principal stress. The vicinity of the fracture front yields a negative singularity of the fluid pressure when the fluid is assumed to reach the fracture front, as in the zero-lag approximation. If the mechanical response is governed by the Linear Elastic Fracture Mechanics (LEFM) and the flow of a Newtonian fluid in the fracture is governed by Cubic's Law, considering linear pressure drop, the fluid pressure behaves as P_f directly proportional to $l_f$in

the finite fracture toughness case, where P_f is the fluid pressure and l_f is the normal distance of the fluid inside the fracture. The fluid driven crack propagates till the pressure applied is high enough to overcome the critical stress intensity factor K_{IC}; i.e. till the stress intensity factor of the crack $K_I < K_{IC}$. The fluid front is assumed to reach the crack tip only under low viscosity conditions. The walls of the crack are loaded by fluid pressure P_f and vicinity by the stress σ_0. The solution of the fluid-driven fracture problem is given by the net fluid pressure $P_{net} = P_f - \sigma_0$, the fracture opening w, the length of the fluid inside the crack and the length of the crack as function of the position x along the fracture (P and w only), time t, and five problem parameters. These parameters are the injection rate q_0, the fluid pressure P_f and the three material parameters, viscosity μ, Young's modulus E and critical stress intensity factor K_{IC}.

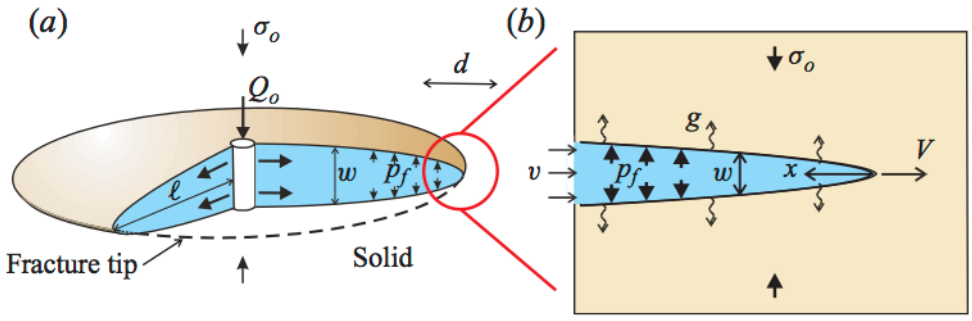

Figure 2.5 Radial flow in hydraulic fracturing with no fluid lag.

Figure 2.6 shows a simple two-dimensional cross-section through an idealized hydraulic fracture. Fracturing fluid enters the wellbore at the center of the fracture, which is assumed to be an ellipse that has extended in a plane normal to the direction of least resistance.

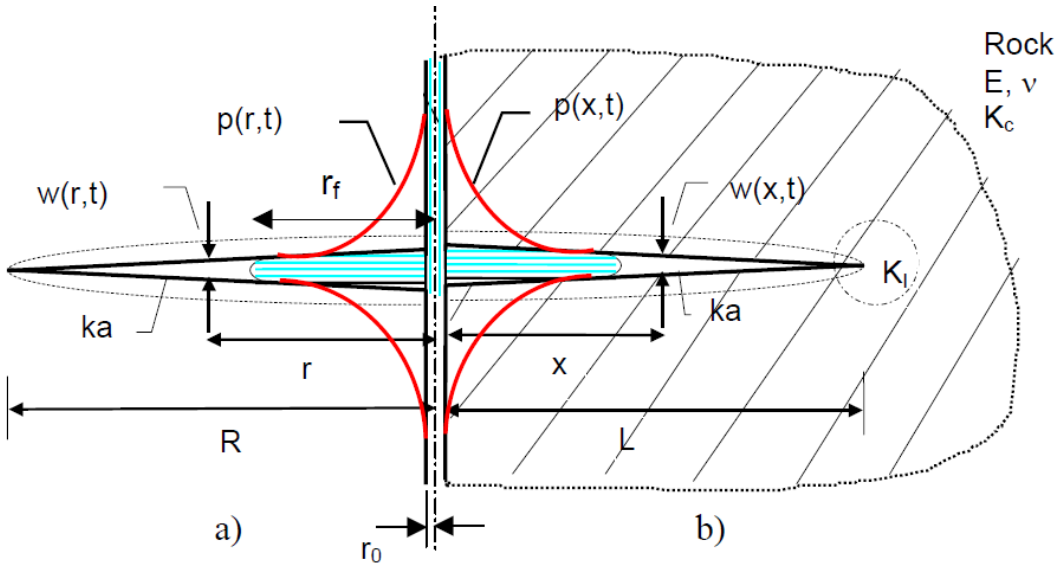

Figure 2.6 Fluid-crack interaction processes, a) penny shaped crack b) wedge shaped crack

As mentioned earlier, fluid pressure and viscosity are the two controlling parameters to crack propagation. For the cavity to exist in front of fluid tip, the fluid needs to have high viscosity which would cause a lag between the crack tip and fluid front. In other words, as the fluid cannot sustain infinite suction at the fracture tip, a cavity devoid of the fracturing fluid has to be naturally present near the crack tip. In the case of an impermeable medium, this void is filled with the

vapors of the fracturing fluid under approximately constant vapor pressure. On the other hand, in the case of a permeable saturated medium, the cavity is filled with the natural gas which is continuously sucked into the fracture at the crack tip and is ejected back into the medium near the fluid fracture interface (Rubin, 1993; Detournay and Garagash, 2003).

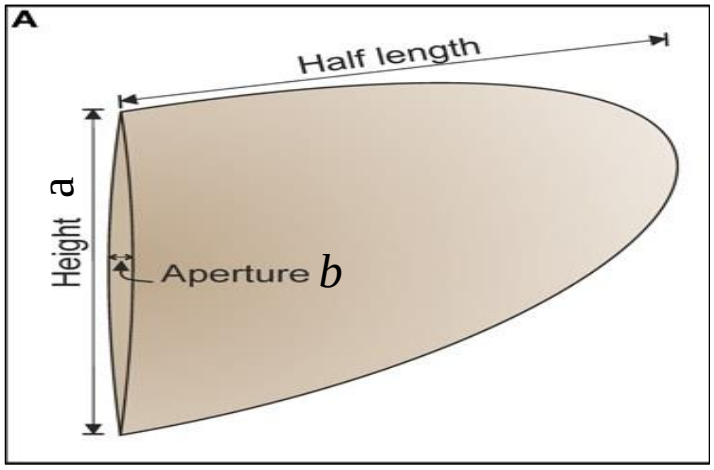

Figure 2.7 Representation of the crack having elliptical opening.

journal.frontiersin.org

Fluid lag results in a tensile stress concentration at the crack tip. Elastic stress concentration at the crack tip increases directly with 2a/b, considering elliptical opening of the fracture, where '*a'* is the major axis and '*b'* is the minor axis of the ellipse as shown in figure 2.7. (Inglis, 1913). The concentration is very high, and the crack will extend for the case of *a*>>*b*, i.e., a 'sharp' crack, as soon as the fluid pressure exceeds the magnitude of the least compressive principal stress and there will be a pressure gradient from the injection point towards the

crack tip as the fluid flows towards the tips. This pressure gradient will depend on the fluid viscosity. Considering rock to exhibit some level of permeability, fluid will also flow (or 'leak–off') into the formation as it flows under pressure along the fracture; the rock has a finite strength, or 'toughness' so that energy will be required for the crack to propagate.

First analytical solution for the stresses in the elastic medium and the crack-opening displacement along the crack was published by Inglis (1913) and served as the basis for early applications to hydraulic fracturing and fracture treatment design. The Perkins, Kern (1961) and Nordgren (1972) (PKN) and Geertsma and de Klerk (1969) (GDK) models are still used, even though numerical models and combinations are now common (Charles Fairhurst, 2013).

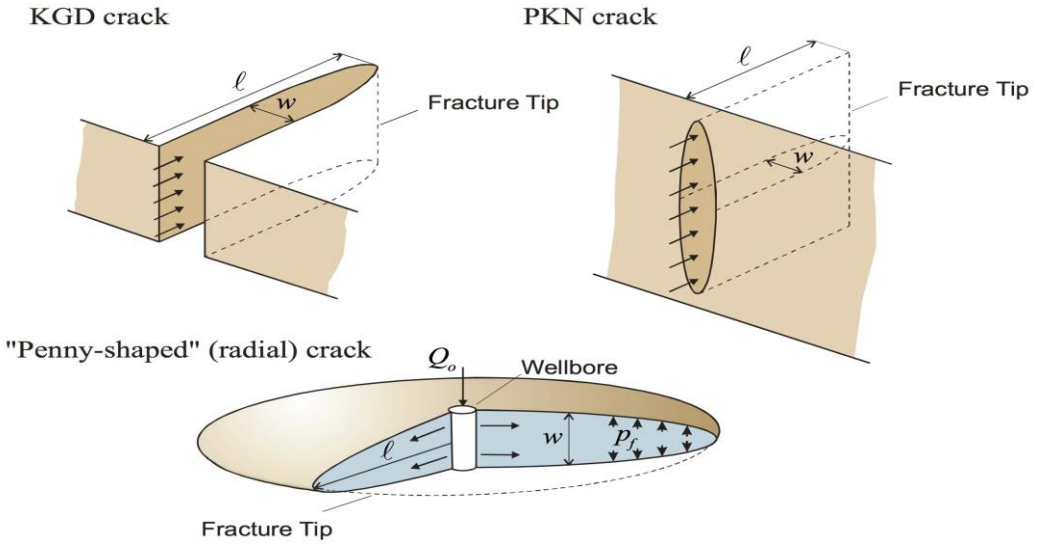

Figure 2.8 The Perkins, Kern (1961) and Nordgren (1972) (PKN) and Geertsma and de Klerk (1969) (KGD) models. www.cefor.umn.edu

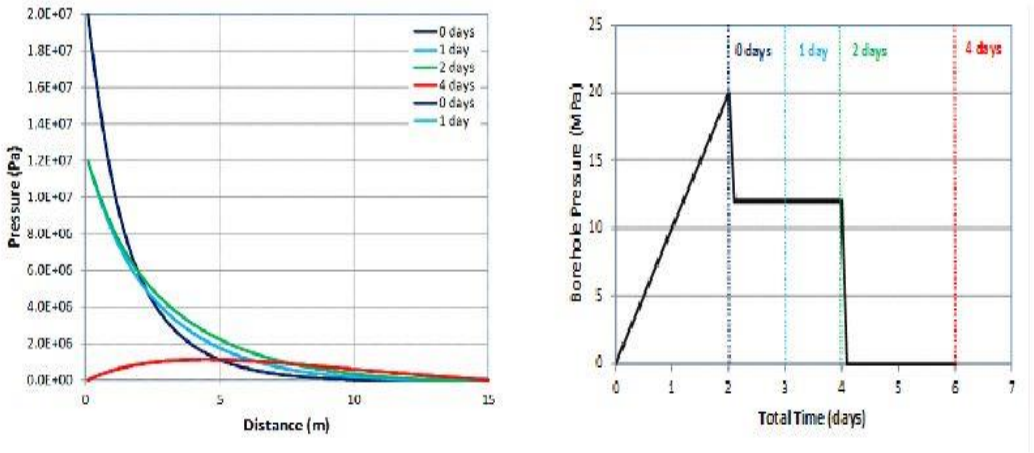

Figure 2.9 Fluid Pressure Distributions along the Central Axis.

www.intechopen.com

Figure 2.9 illustrates that the fluid pressure in a permeable rock can continue to flow away from the point of injection even after the borehole pressure is reduced to zero. The pressure vs time graph (right) shows the distribution of fluid pressure in the rock mass after (i) 2 days of pressurization up to the peak pressure of 20 MPa in the fracture; (ii) stop pumping and reduce fluid pressure quickly to 12MPa at the point of injection; (iii) hold the pressure constant for 2 days; and (iv) drop the pressure to zero.

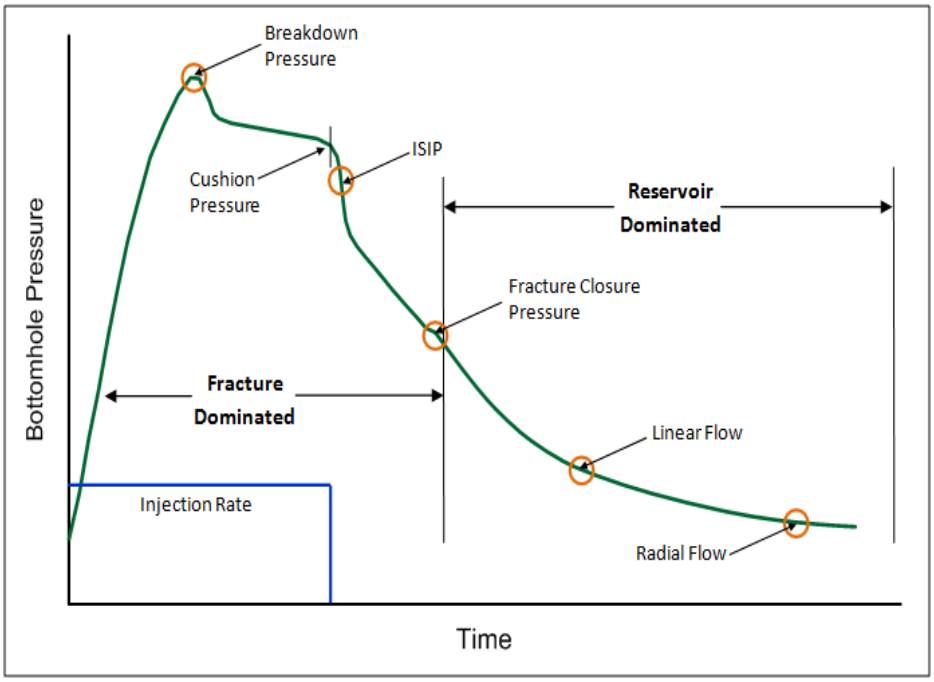

Figure 2.10 Pressure required over time for hydraulic fracturing.

http://www.fekete.com

Figure 2.10 explains the pressure required to break open the rock and continue keeping it open. Different combinations of rock permeability, injection rates and extents can lead to higher peak pressure values in the rock. The drop in Instantaneous Shut in Pressure (ISIP) explains that the far field stresses trying to shut the opened fracture. Fracture surface rests on the proppant injected into the cavity keeping the fracture open and allowing the fluid to flow with minimum pressure drop. Such flow may contribute to slip on pre-existing fractures after the pressure in the borehole is reduced to zero.

Chapter 3

MODELING FLUID-DRIVEN CRACK GROWTH

3.1 General Description

The Boundary Element Method (BEM) approach is applied to the solve problem of fluid flow and fracture propagation. The numerical BEM model of hydraulic fracture propagation will be used to calculate results. Additionally, an explicit crack representation is used to update the crack during propagation. This explicit representation is applied to a fluid-filled crack in an impermeable, elastic solid and compared to the plane-strain hydraulic fracture problem with a fluid lag.

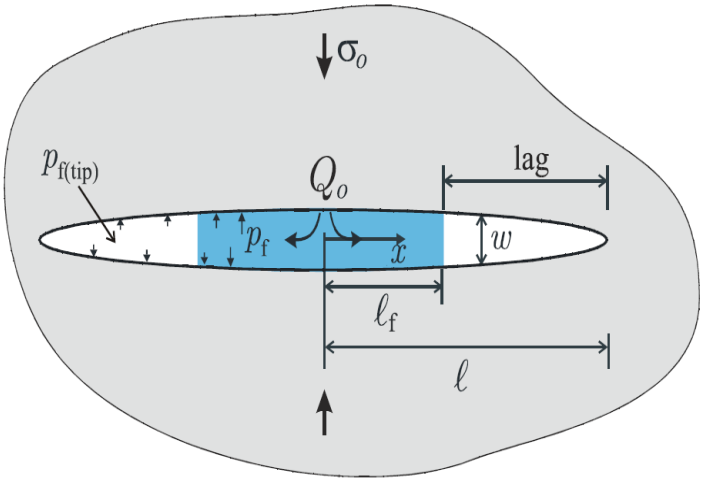

Figure 3.1 Two-dimensional fluid-driven hydraulic fractures with fluid lag. Garagash, Dmitry I. "Propagation of a plane-strain hydraulic fracture with a fluid lag: Early-time solution." International journal of solids and structures 43.18 (2006): 5811-5835.

When fracturing fluid, having viscosity μ, is injected within the fracture, imposes a pressure load on the fracture surfaces walls. As a result, the rock undergoes a mechanical deformation and the fracture starts to propagate when a critical condition is reached. From the previous study it is understood that, higher the viscosity, greater is the fluid lag.

Subject to the different modeling assumptions, this critical condition can be defined by stress intensity criterion. The following assumptions are usually made for the hydraulic fracture model:

I) The fluid flow is governed by the lubrication theory,

II) Solid deformation is modeled using the theory of linear elasticity,

III) The propagation criterion is given by the stress intensity approach of linear elastic fracture mechanics (LEFM) theory.

3.1.1 Fluid flow in the fracture

The fluid filed part of the fracture is governed by the lubrication theory; i.e. by the local and global continuity equation and Cubic's law. As mentioned earlier the equation for the fluid flow is given by

$$Qx = -\frac{h^3}{12\mu}\frac{dP}{dx} \tag{15}$$

Equation (15) is valid between $0 \leq x \leq l_f$. Pressure in the lag zone is given by,

$$P_{lag} = P_{tip} \qquad l_f \leq x \leq l \tag{16}$$

3.1.2 Fracture propagation

The crack propagates when the mode I stress intensity factor reaches the fracture toughness i.e. when the critical stress intensity factor is greater than the rock toughness $K_{Ic} \geq K_I$. (N. Weber, P. Siebert, K. Willbrand, M. Feinendegen, C. Clauser and T. P. Fries, 2013).

3.2 Governing Equations for single crack geometry

Consider a single two-dimensional plan strain fluid driven fracture Γ propagating in homogeneous, isotropic, linear elastic, impermeable medium Ω, see Figure 3.2. The boundary of the domain consists of Γ_F on which prescribed tractions τ are imposed, Γ_u on which prescribed displacements are imposed, and fracture faces Γ_c subject to fluid pressure.

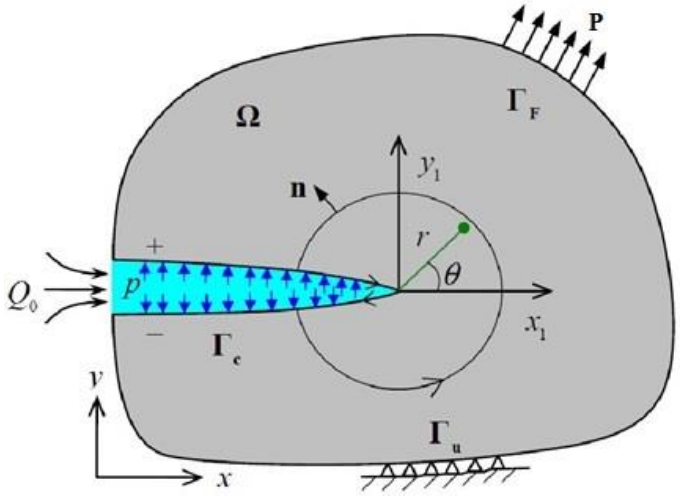

Figure 3.2 A homogenous, isotropic, linearly elastic body Ω with piecewise smooth boundary Γ in equilibrium. www.intechopen.com

The fracture propagation is driven by injection of an incompressible Newtonian fluid at constant volumetric rate q_0. It is assumed that the fracture is filled with fluid with some lag from crack tip; i.e. the fluid has high viscosity. The solution of the problem consists of determining the growth of the fracture length l, the fluid length l_f as well as the height of the fracture opening ω, the fluid pressure P_f, deformations and stresses inside the domain as functions of both position and time. The stresses inside the domain, σ and τ, are related to fluid pressure P_f and the displacement u through the stress- displacement equilibrium equation, given by,

$$\sigma_{ij} = -P\delta_{i,j} + \mu\left(u_{i,j} + u_{j,i}\right) \tag{17}$$

where, σ_{ij} is the stress tensor component in i and j direction, P is the hydrostatic fluid pressure, μ is the dynamic viscosity and u is the displacement component. The traction is applied to the outer boundary, equal in magnitude but opposite in direction and is represented as,

$$\sigma.n = \hat{t} \tag{18}$$

Consider a surface with small element on the boundary and it is assumed that the normal component of the traction acting on the surface is the pressure component as shown in figure 3.2. The shear component of the traction is assumed to be zero.

$$\sigma_x = -P \tag{19}$$

$$\sigma_y = -P \tag{20}$$

Equation (19) and (20) shows the stresses acting in x and y direction inside the fracture. As shown in figure 3.3, it is assumed that the shear stress component τ^+ and τ^- acting on the fracture surface, equal in magnitude but in the direction opposite to fracture propagation is given by,

$$\tau^+ = -\mu(4\,\frac{V_{x0}}{\omega_n}) \tag{21}$$

$$\tau^- = \mu\left(4\,\frac{V_{x0}}{\omega_n}\right) \tag{22}$$

Where, V_{x0} is the velocity of the fluid at point of entry into the fracture and ω_n is the fracture opening at that point. The equation for fluid velocity is given by,

$$V_x = V_{x0}\left(1 - 4\,\frac{y}{{\omega_n}^2}\right) \tag{23}$$

Where, V_x is the fluid velocity at any point inside the crack domain and V_{x0} is the fluid velocity at crack inlet point. The flow rate at any point is calculated by integrating the velocity profile over the opening of the crack and is given by the equation.

$$q = \int_{-\frac{\omega_n}{2}}^{\frac{\omega_n}{2}} V_x dy = \frac{2}{3} V_{x0}\omega_n \tag{24}$$

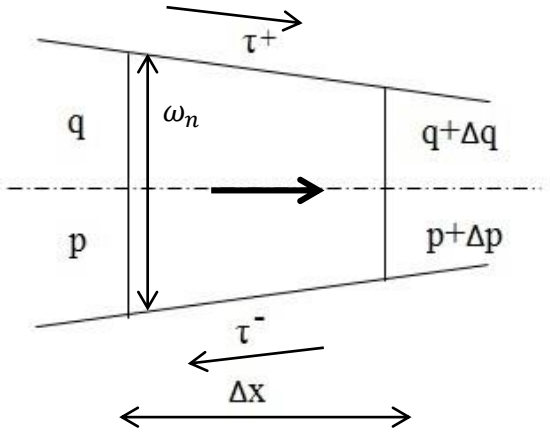

Figure 3.3 Fluid pressure, Flow rate, and stress component inside the crack

The fluid is injected into the fracture at a constant rate q_0. Considering impermeable solid, the leak-off is negligible and therefore considered zero. It is assumed that a fluid lag develops between the fluid front l_f and the crack tip. (N. Weber, P. Siebert, K. Willbrand, M. Feinendegen, C. Clauser and T. P. Fries, 2013). However, for simplicity the fluid lag is not considered as the part of the equation (24). The boundary conditions for the fluid flow problem are as follows:

$$q = q_f \quad \text{at the fluid front}$$

The flow condition at the fluid front q_f is determined from the pressure gradient and thus, is part of the solution. The pressure in the lag region is set to zero.

$$p = 0 \qquad \text{in the fluid lag}$$

The equilibrium equation is given by,

$$\lambda(P\omega_n)_x = \tau^+ - \tau^- = -8\mu \frac{V_{x0}}{\omega_n} = -12\,\mu\,\frac{q}{{\omega_n}^2} \quad (25)$$

Assuming λ =1,

$$(P\omega_n)_x = -12\,\mu\frac{q}{{\omega_n}^2} \quad (26)$$

The mass conservation equation is given by,

$$q_x + \omega_n * = 0 \quad (27)$$

From equation (26) and (27) we get the first governing equation, represented as,

$$(\frac{{\omega_n}^2}{12\mu}\,(P\omega_n)_x)_x = \omega_n * \quad (28)$$

Equation (28) explains, when fluid having pressure P and viscosity μ, is injected into the fracture, causes the fracture profile to open by ω_n. The crack tip is taken as the last node in a quadratic discontinuous element, and the displacement discontinuity at the crack tip node is assigned to be zero, as shown in Fig. 3.4.

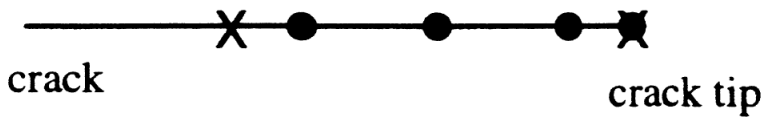

Figure 3.4 Discontinuous crack tip element. Yang, B., and K. Ravi-Chandar. "Evaluation of elastic T-stress by the stress difference method." Engineering Fracture Mechanics 64.5 (1999): 589-605.

The regular finite difference polynomial interpolation is applied to all the elements including the crack tip element and the other quadratic discontinuous elements along the boundary and the crack. (B. Yang, K. Ravi-Chandar, 1999)

The numerically obtained crack opening displacement profile is given by,

$$\left[\frac{{\omega_n}^2}{12\mu}\,(P\omega_n)_x\right]_{i+\frac{1}{2}} - \left[\frac{{\omega_n}^2}{12\mu}\,(P\omega_n)_x\right]_{i-\frac{1}{2}} = \frac{\frac{(\omega_{ni}+\omega_{ni+1})^2}{2}}{12\mu}\,\frac{(P_{i+1}\omega_{ni+1}-\omega_{ni}P_i)}{x_{i+1}-x_i} - \frac{\frac{(\omega_{n-i}+\omega_{ni})^2}{2}}{12\mu}\,\frac{(P_i\omega_{ni}-\omega_{ni-1}P_{i-1})}{x_i-x_{i-1}} \tag{29}$$

The Finite Difference Method (FDM) requires calculations on nodes that include the entire domain. FDM, mainly used in fracture mechanics is mostly limited to dynamic fracture propagation and dynamic stress intensity factor calculation.

(Zuorong Chen, 2013) in his paper made the assumptions of small strains and displacements, the kinematic equations, which include the strain-displacement relationship, the prescribed displacement boundary conditions and the crack surfaces separation, which reads,

$$\omega = u^+ - u^- \tag{30}$$

where, u^+ & u^- are displacements on either side of the crack surface. As mentioned earlier that fluid lag creates high stress concentration at the crack tip, forming a sharp crack tip, the boundary integral element method cannot be used to

produce boundary element method directly. A number of problems have been addressed using cracks Green function. A similar approach has been applied in this study. Furthermore, we neglect all body forces for our simplicity. This results in the following sets of equations for the displacement and traction components.

$$P_i = \oiint u_{ij}^* P_j - P_{ij}^* u_j dp + \oiint P_{ij}^* \omega_j dp \quad (31)$$

Where P_i is the hydrostatic pressure acting in the *i*th direction, u_{ij}^* and P_{ij}^* are the known Greens functions for displacement and traction respectively. P_j is the normal component of traction in the *j*th direction, u_j being the displacement component in the *j*th direction and ω_j is the component for aperture opening. Equation (28) and (31) form a set of governing equations to be solved for two unknowns, pressure *P* and crack opening $\omega_n *$.

Chapter 4

SIMULATION AND RESULTS

4.1. Numerical algorithm

The simulation process is carried out through an iterative combination of the fluid flow and solid body deformation. Starting with an initial solution and an estimate value for the fluid flow, the pressure gradient and the crack opening are calculated until the solution is converged. When the propagation condition is met ($K_{Ic} \geq K_I$), the crack propagates to the next node. Else, the fluid front is moved towards the crack tip with a velocity V_x determined from the fluid flow rate q.

In figure 4.1, $u^+ \,\&\, u^-$ shows the displacement of the crack walls perpendicular to the direction of the crack propagation, indicating the opening of the crack profile. A simple flow chart shown below explains the crack and fluid moving mechanism, propagating simultaneously under loading condition.

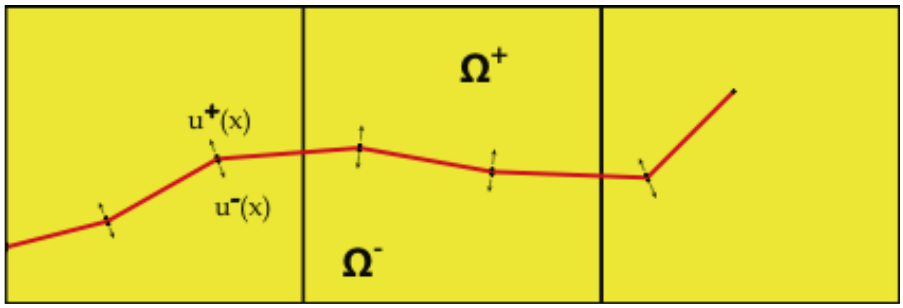

(a)

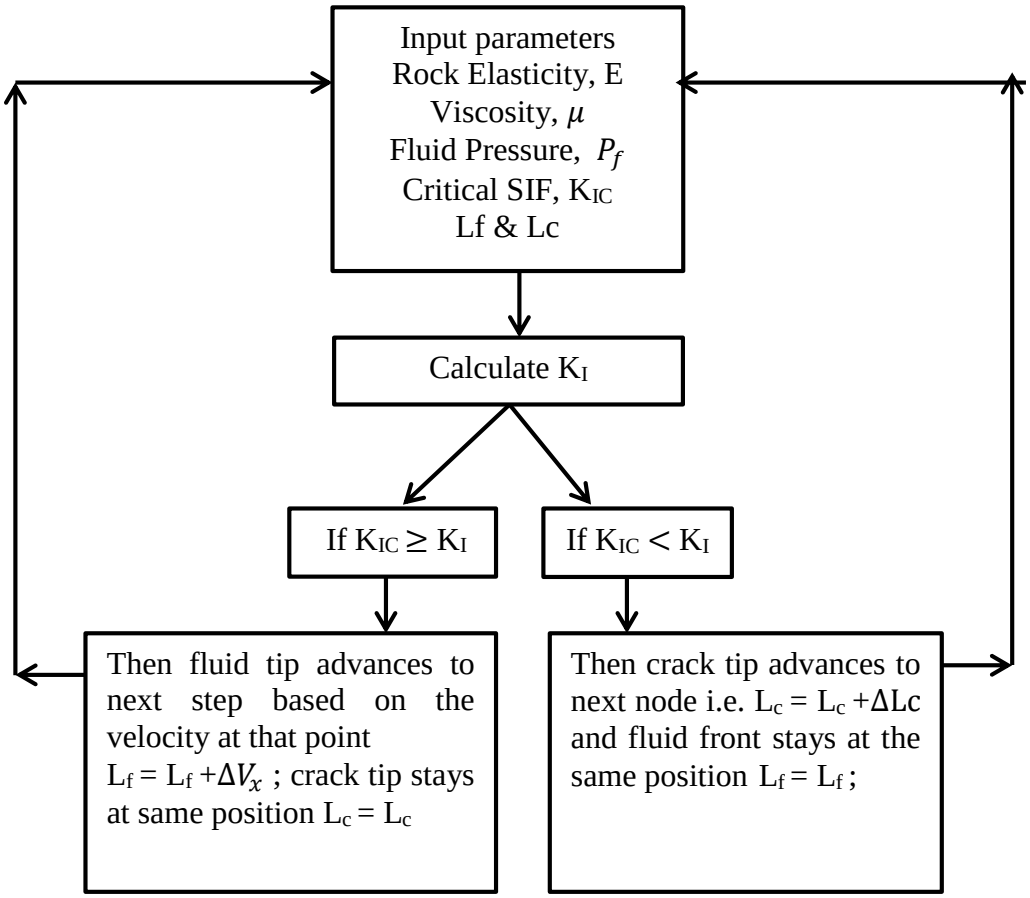

(b)

Figure 4.1 (a) Interpolation of crack opening along the domain.

http://www.intechopen.com (b) Flowchart of code

It is necessary to understand the physics behind crack propagation. When the pressurized fluid, having viscosity, is injected into the crack, the viscous forces tend to push the walls of the crack in the outward direction, thereby opening the fracture. A highly viscous fluid creates a lag and this creates high stress concentration region at the crack tip. Because of the high pressure, acting at the crack tip, the crack propagates to the next step and will propagate till $K_{IC} \geq K_I$. Once SIF falls below the critical SIF, the crack stops propagating and the fluid front starts advancing to the next element, till the crack is pressurized again and $K_{IC} \geq K_I$.

4.2. Numerical results

For simplicity the parameters are normalized and normalizing factor is taken to be 10^6. Let us consider the length of the fracture $L_0 = 1m$, the young's modulus of the rock to be $E_0 = 1$kPa and viscosity $\mu_0 = 10^6\ Pa\,.s$. Hence after normalizing the parameters become

$$\mu = \underset{\mu}{\rightarrow} \mu_0\ ,\ \ \sigma = \underset{\sigma}{\rightarrow} E_0\ , E = \underset{E}{\rightarrow} E_0\ ,\ L = \underset{L}{\rightarrow} L_0\ , t = \underset{t}{\rightarrow} \frac{\mu_0}{E_0}$$

The numerical results for the crack opening and pressure distribution at the wellbore of a plane-strain hydraulic fracture problem are calculated (N. Weber, P. Siebert, K. Willbrand, M. Feinendegen, C. Clauser and T. P. Fries, 2013). The stress intensity factor K_{IC} is given by $K_{IC} = \underset{K_{IC}}{\longrightarrow} E_0\sqrt{L_0}$ and is taken to be $10^6\ Pa\ \sqrt{m}$. The boundary condition of zero displacement at crack tip is

approximated by finite elements and a local mesh in the area close to the crack interface. Computational data of the validity of approximating the finite medium with a finite block is provided in (Hunsweck, M. J, Shen, Y, & Lew, 2012)

The selection of fracturing fluid varies from company to company. It depends on the volume of the site under consideration and then this is followed by how much viscosity is needed to provide sufficient fracture width to ensure proppant into the fracture. Also to provide a desired net pressure to control the crack propagation process. The material properties mentioned by (Dimitry Chuprakov) in his paper are used as input for numerical analysis.

Table 4.1 Material Properties

Parameter		Range
Q	Volumetric Injection Rate	0.01-0.25 m^3/s
L	Distance between HF and NF	1-10m
μ	Fluid Viscosity	1-1000cp
E	Young's modulus	9-110GPa
ϑ	Poisson's Coefficient	0.11-0.252
K_{IC}	Mode I fracture toughness	0.1-2.7MPa.$m^{1/2}$
σ_1	Maximum in-situ stress	13-105 MPa
σ_2	Minimum in-situ stress	11-100MPa

Based on the above material properties and the input parameters given to the algorithm, Figure 4.2 shows the meshed fracture model.

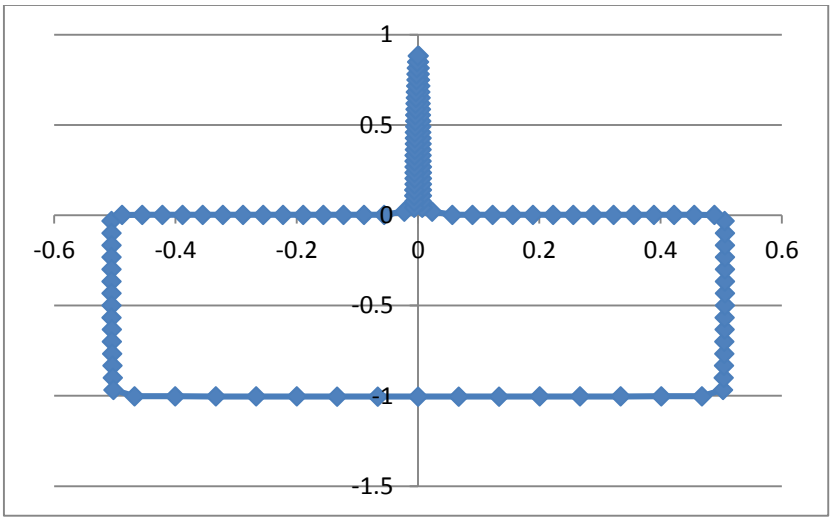

Figure 4.2 fracture geometry when 1MPa pressure is applied

The results were obtained by taking rock elasticity (E) as 50GPa, Viscosity μ as 500cp and the critical stress intensity factor K_{IC} was chosen to be $1\ Pa\sqrt{m}$. Effect of different pressure values on crack propagation and crack opening was studied.

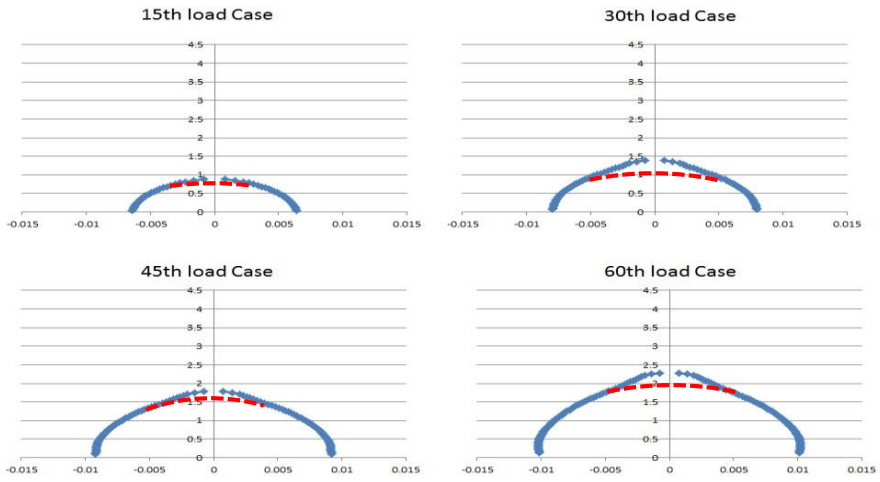

(a)

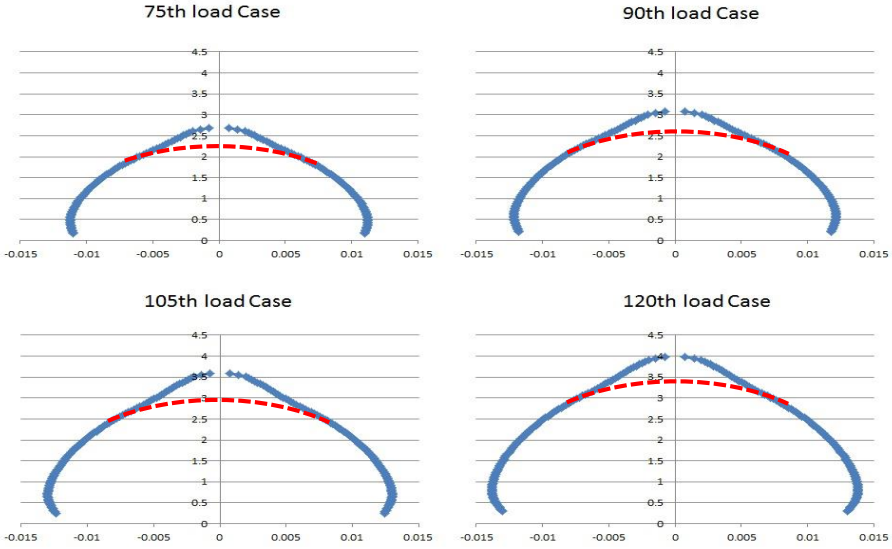

(b)

Figure 4.3 Crack propagating under pressure of 1 MPa (a) for 15th to 60th load case (b) for 75th to 120th load case

As seen in figure 4.3a load case 15th, there is almost negligible fluid lag. A high stress concentration region is formed at the crack tip as the fluid keeps on pressurizing the crack walls. To release this pressure, the crack tip propagates to the next node and it continues to propagate till the stress intensity factor (K_I), calculated from the pressure applied, falls below the critical SIF (K_{IC}). Once the crack propagation stops, the fluid front follows to the next step by the same amount as the velocity at that step. A noticeable fluid lag can be seen in the 30th load case as the crack propagates ahead. The lag is again reduced in 45th load case as the fluid front moves ahead and the cycle continues till the pressure applied is no capable of making the crack propagate further.

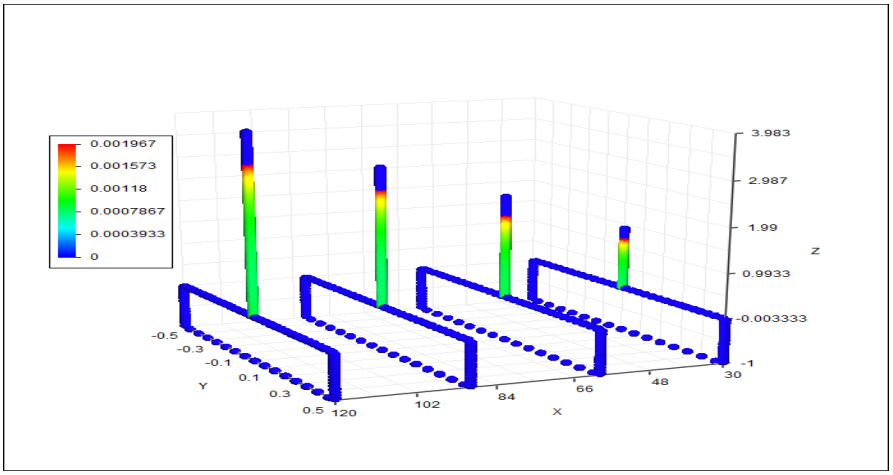

Figure 4.4 Velocity Profile of the fluid inside the fracture geometry when 1MPa pressure is applied

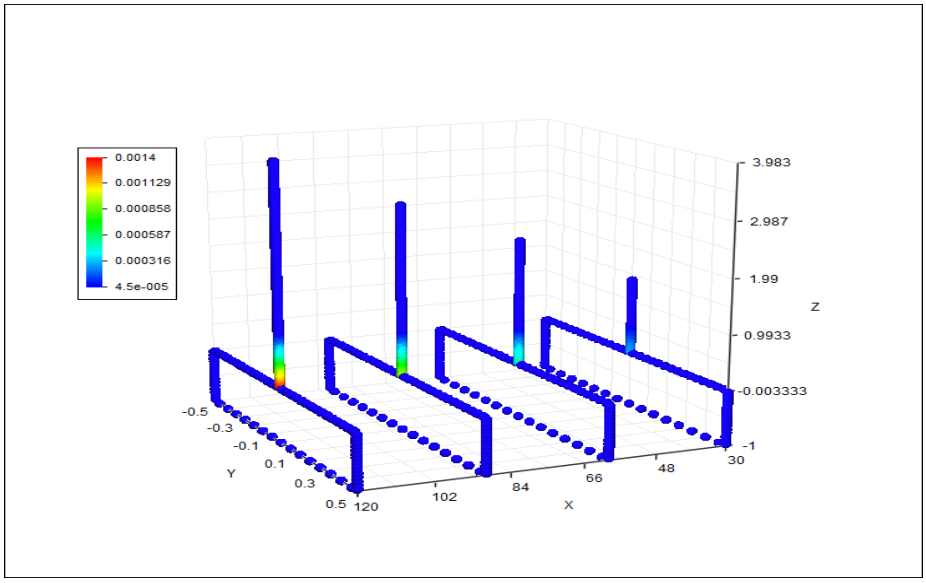

Figure 4.5 Crack Opening Profile of the fracture geometry

The fluid crack interaction phenomena can be visualized in figure 4.4 and 4.5. Figure 4.4 represents the velocity profile of the fluid inside the crack geometry. The *x* axis represents the load cases, the *y* and *z* axis represents the geometry size. The blue rectangular region in the figure 4.4 represents the drilled wellbore into which, the pressurized fluid is injected. The velocity of the fluid is the highest at the tip as it is continuously pressed from the fluid following it.

Figure 4.5 explains the crack opening profile when the fluid enters the crack. It can be seen that, initially the crack isn't opened much but as the crack and fluid advances, the walls of the crack are pressurized by the viscous forces of the fluid, which causes the fracture to open up and allows more fluid to enter the fracture thereby increasing the velocity.

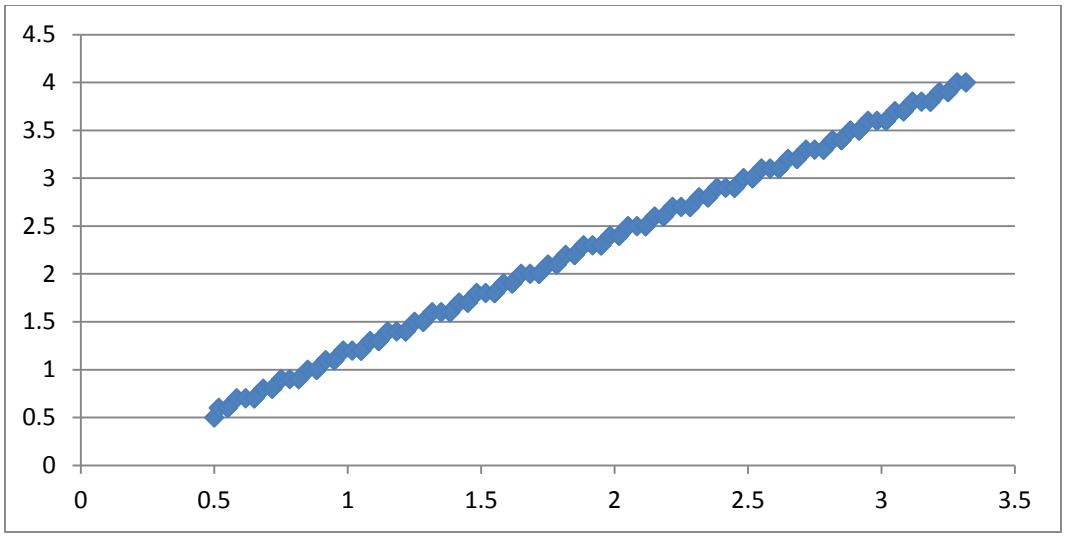

(a)

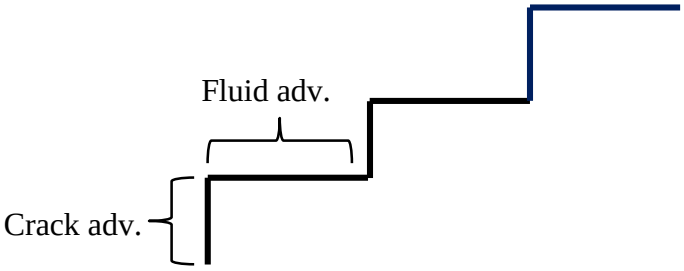

(b)

Figure 4.6 (a) Graph of Fluid tip Vs. Crack tip. (b) Fluid tip advancement Vs. Crack tip advancement

As mentioned above, initially as the fluid enters the crack, it starts pressurizing the walls and creates a high stress region at the crack tip making it impossible for the crack to sustain without propagating. Hence the crack advances, followed by the fluid as the crack advancement creates more volume

for the fluid to flow in. The graph goes on increasing gradually and gives us the estimate of how far the crack would propagate under applied pressure.

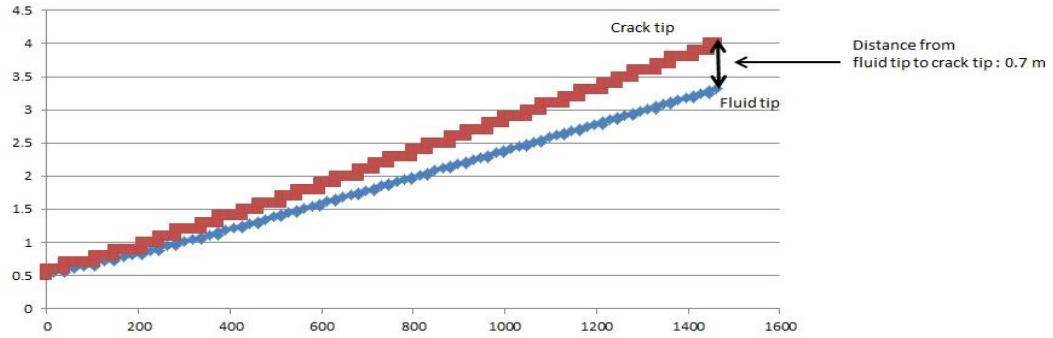

Figure 4.7 graph showing distance between fluid tip and crack tip (fluid lag) when pressure of 1MPa is applied**.**

From figure 4.7, it can be concluded that as the time advances the fluid lag increases gradually as seen in figure 4.3a and 4.3b. From the above graph at the end of 120th load case it is found that the fluid lag is about 0.7 m.

In the second example, pressure of 2MPa was applied to the fracture geometry. A noticeable difference was noticed in the behavior of the fracture propagation. Based on the input parameters taken to be 50GPa rock elasticity, 500cp viscosity and 2MPa pressure the fracture model generated is shown in figure 4.8. It can be seen that the crack opening has been widened as compared to the fracture model when 1MPa pressure was applied.

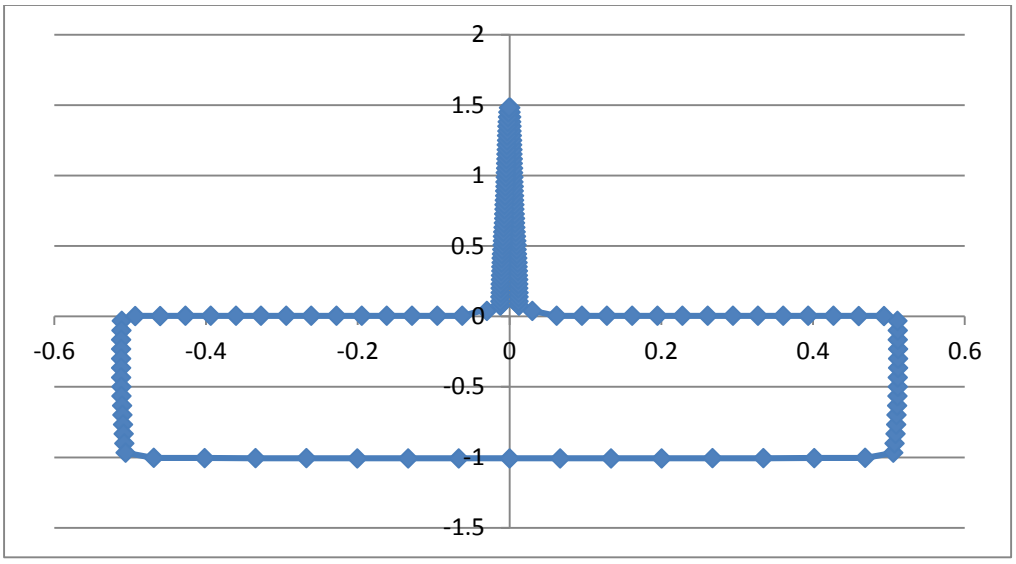

Figure 4.8 fracture geometry when 2MPa pressure is applied

As compared to the 15th load case of previous example, the crack seems to have propagated by 0.5m because of the increase in the pressure and also because of more driving force. The fluid entering the crack pressurizes the walls, which causes the crack to open up and additional fluid flows in. Effective stress intensity factor at the crack tip is more than the critical SIF and hence crack continues to propagate more than the previous example. As explained earlier that the fluid front does not move till the crack stops advancing. In the 75th load case, a curve at the crack opening can be observed. At this instance, fluid pressure keeps on increasing on the walls and causes it to deform till the pressure is released and fluid starts propagating.

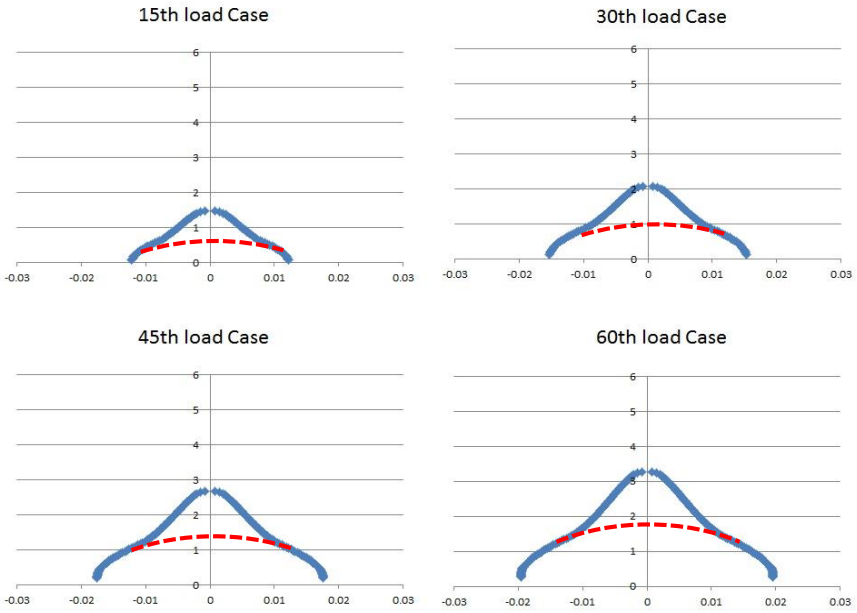

(a)

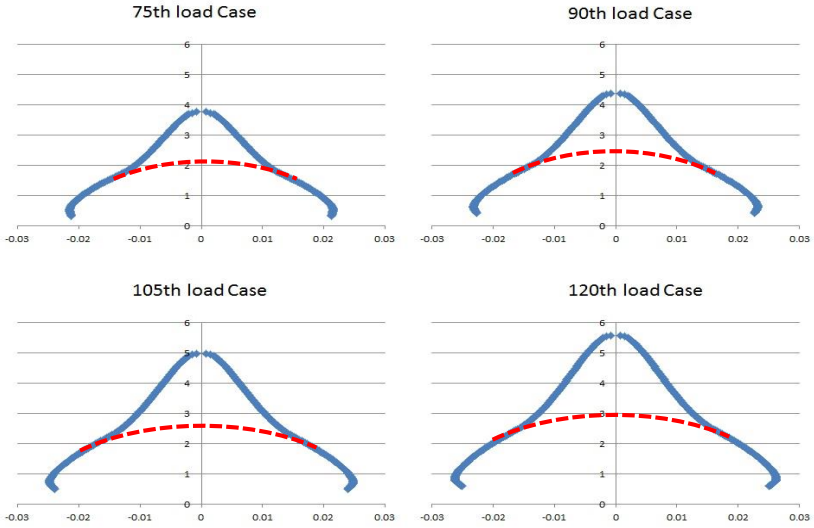

(b)

Figure 4.9 Crack propagating under pressure of 2 MPa (a) for 15th to 60th load case (b) for 75th to 120th load case

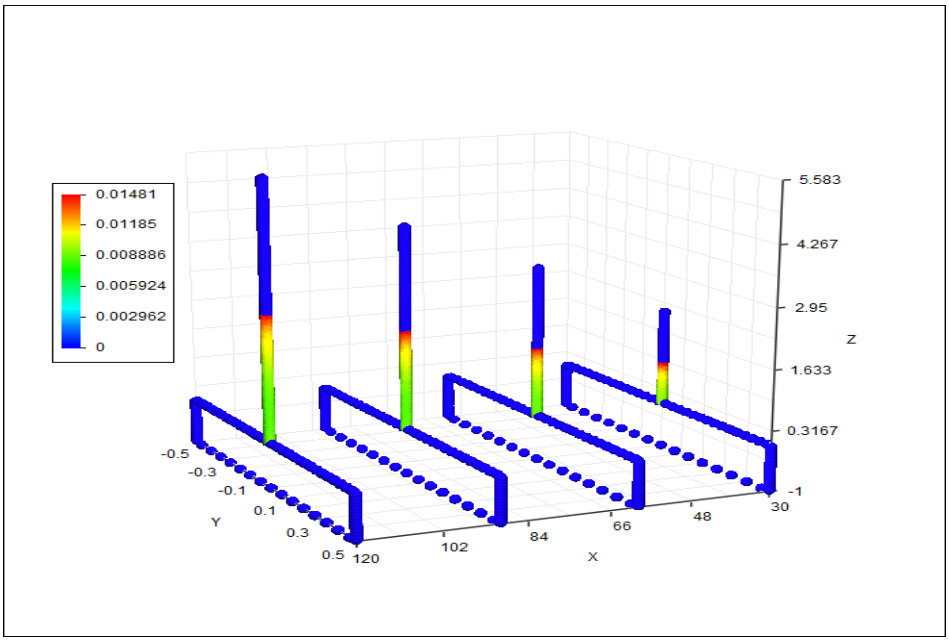

Figure 4.10 Velocity Profile of the fluid inside the fracture geometry

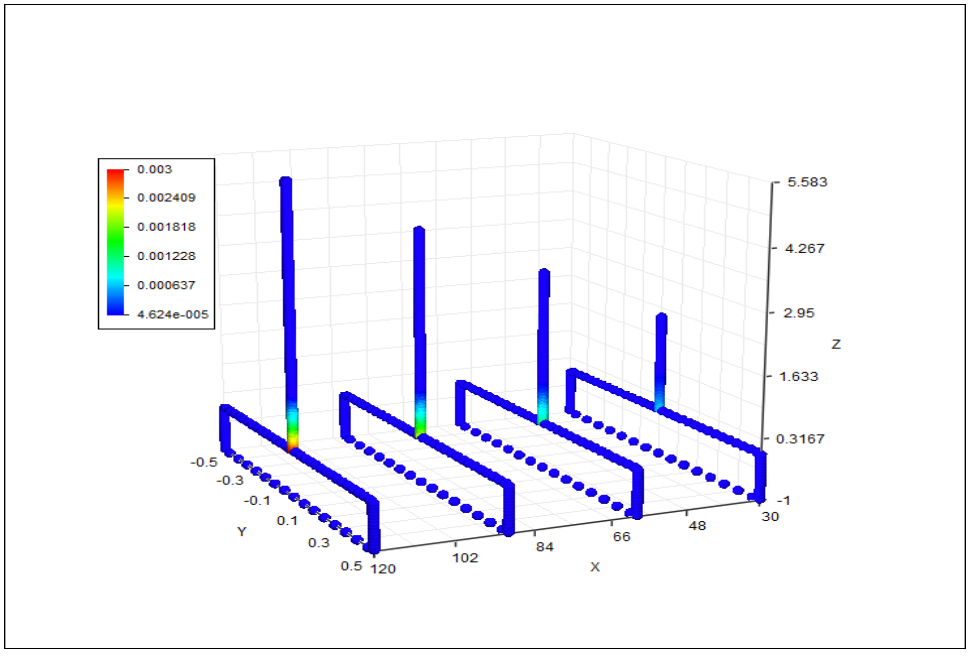

Figure 4.11 Crack Opening Profile of the fracture geometry

The velocity profile as shown in figure 4.10, shows 87% increase in the velocity of the fluid flowing under 2MPa pressure than in the previous example. Interestingly, it can be noticed that the distance between the crack tip and the fluid tip is also increased. That's because of higher effective stress intensity factor which causes the facture to advance more than the fluid front. Figure 4.11 shows the crack opening profile of the geometry. The crack is opened by 53% from the previous case. This increase benefits the crack opening as more fluid enters the fracture, allowing more proppant to flow in to keep the crack open.

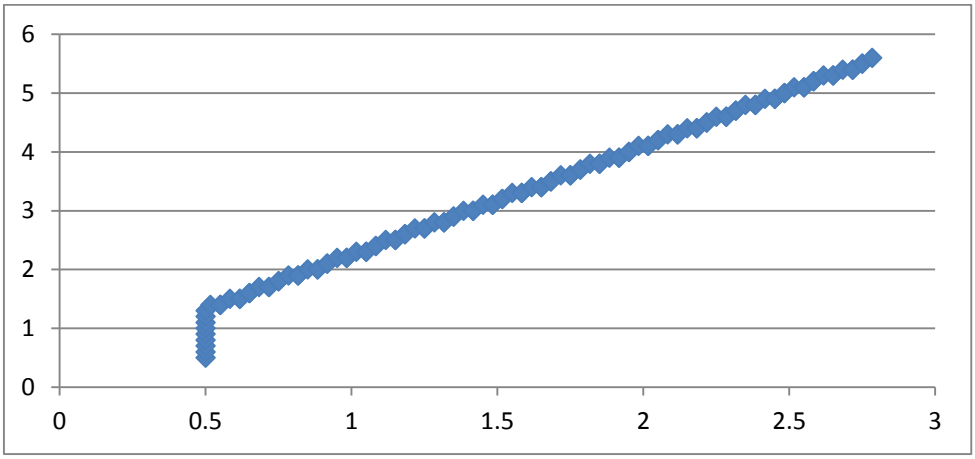

Figure 4.12 Graph of Fluid tip Vs. Crack tip

In figure 4.12, sudden rise in the crack tip explains the distance required to overcome the fluid pressure and also critical stress intensity factor, to stop the crack advancement. Once the initial crack advancement stops, further, the crack and fluid advances gradually.

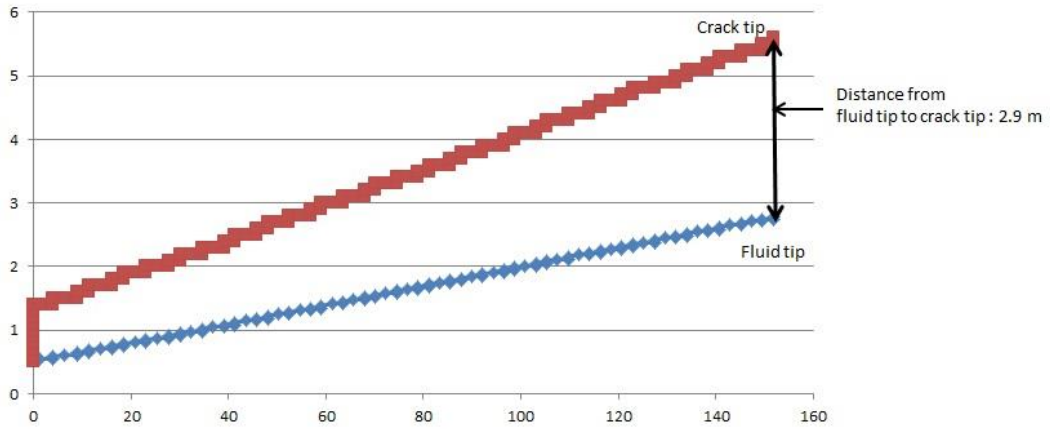

Figure 4.13 Graph showing distance between fluid tip and crack tip (fluid lag) when pressure of 2MPa is applied.

From figure 4.13, it can be concluded that as the time advances the fluid lag increases gradually as seen in figure 4.9a and 4.9b. From the above graph at the end of 120th load case it is found that the fluid lag is about 2.9 m. Also With the increase in pressure the crack length increases, the fracture opening increases and the overall time reduces.

In the next example, pressure of 3MPa was applied to the fracture geometry. Based on the input parameters taken to be 50GPa rock elasticity, 500cp viscosity and 3MPa pressure the fracture model generated is shown in figure 4.14. More widened fracture geometry was observed.

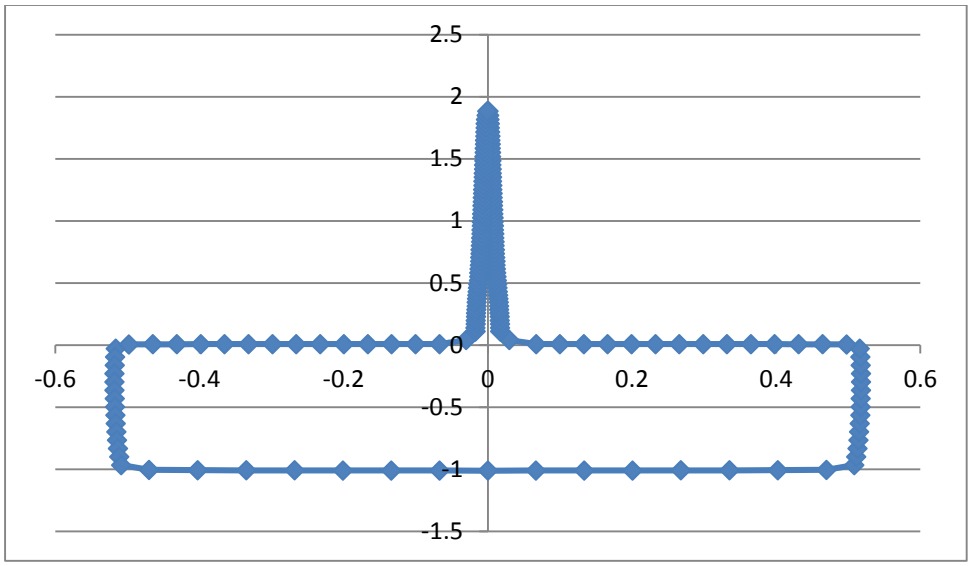

Figure 4.14 Fracture geometry when 3MPa pressure is applied

As per figure 4.15a and 4.15b, crack seems to propagate for 3.5m followed by the fluid front. As the crack advances further, the effective stress intensity factor at the crack tip is adequately higher than the critical SIF and hence crack continues to propagate more than the previous examples and the fluid front halts during that instance. It is observed that the pressure applied is large enough to keep the crack propagating for longer distance. It is evident from the above example that higher pressure causes the width of the fracture to increase, thereby allowing more quantity of proppant to enter the crack and keep the crack open for extracting natural gas. Another benefit of having a wide crack is, increase in the volume of the fluid flowing inside the crack which makes the crack to create a more complex crack network.

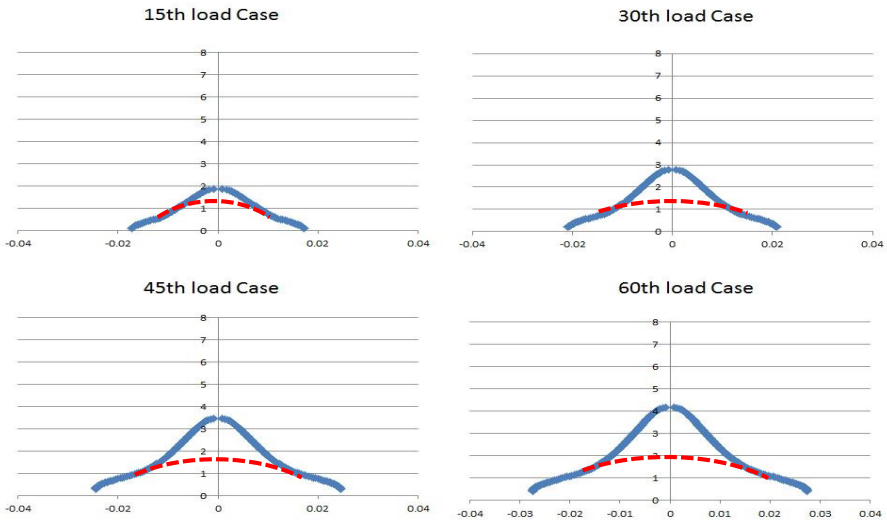

(a)

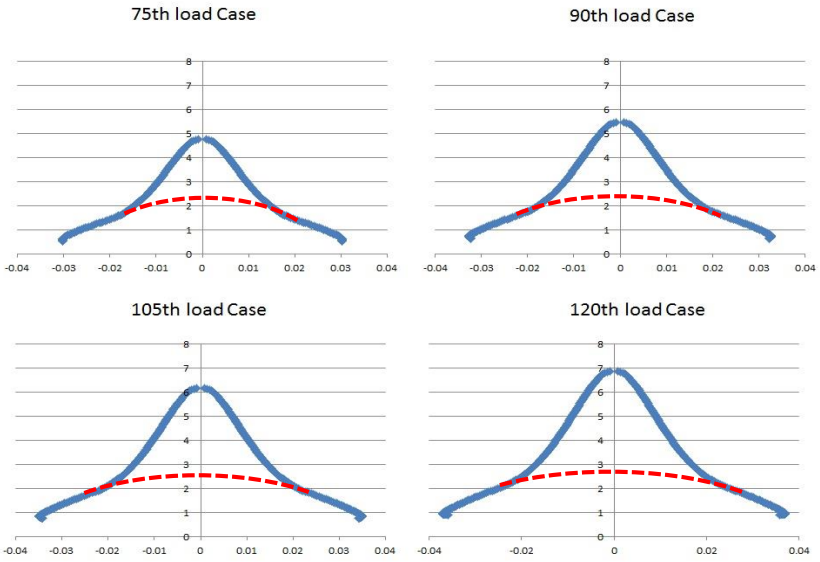

(b)

Figure 4.15 Crack propagating under pressure of 3 MPa (a) for 15th to 60th load case (b) for 75th to 120th load case

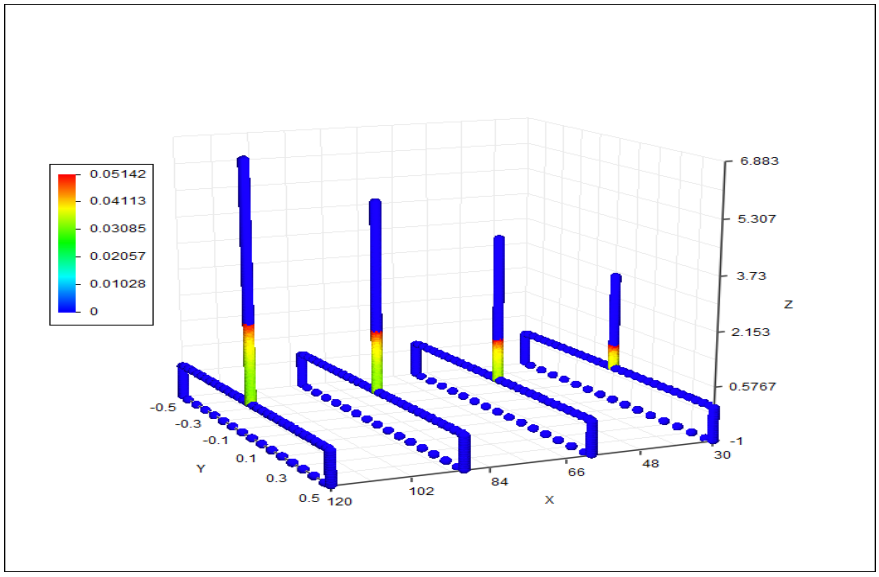

Figure 4.16 Velocity Profile of the fluid inside the fracture geometry

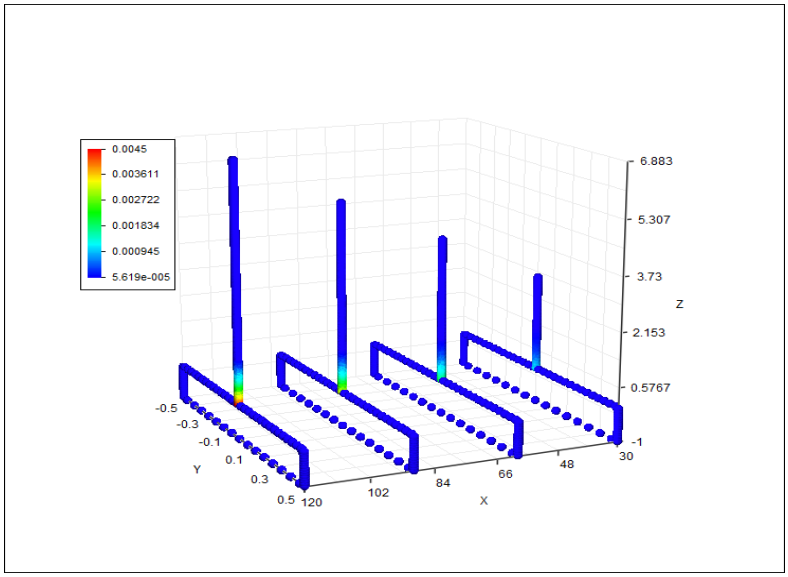

Figure 4.17 Crack Opening Profile of the fracture geometry

The fluid lag phenomena can be visualized from figure 4.16. The figure shows 80% increase in the velocity of the fluid flowing under 3MPa pressure than in the

previous example. That's because of higher effective stress intensity factor which causes the facture to advance more than the fluid front. Figure 4.17 shows the crack opening profile of the geometry. The wide opening of the facture is because of the high pressure applied on the walls of the fracture.

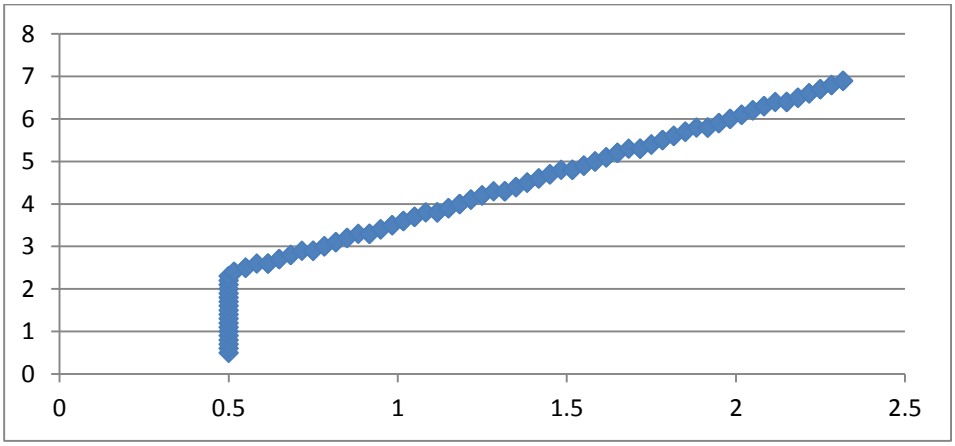

Figure 4.18 Graph of Fluid tip Vs. Crack tip

A steep rise in the above graph represents the crack advance when a pressure of 3MPa is applied to it. In the above graph it can be seen that as the fluid tip travels up to 2.4m into the fracture, the crack tip advances up to 7m. A considerable fluid lag is noticed and is best visualized in figure 4.19 below.

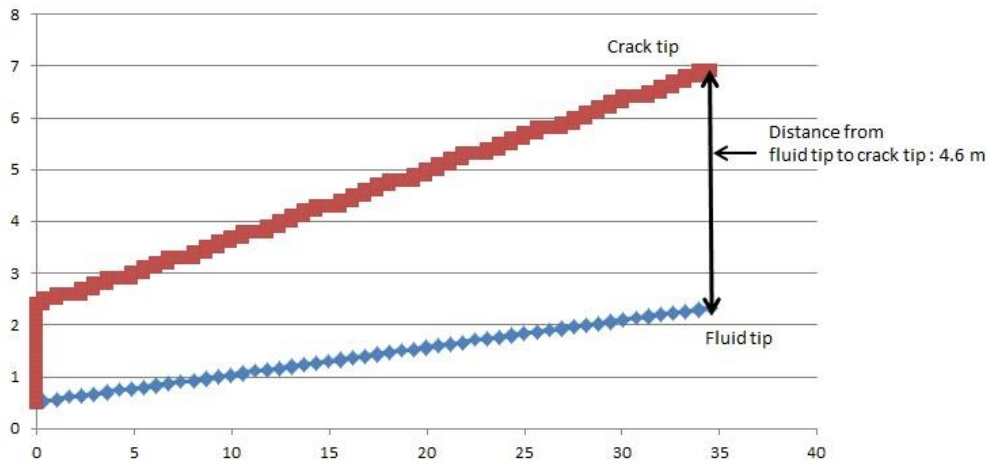

Figure 4.19 Graph showing distance between fluid tip and crack tip (fluid lag) when pressure of 3MPa is applied

Initial advancement of the crack signifies the highly pressurized fluid entering the fracture, giving it enough driving force for propagation. The gradual increase between the fluid tip and the crack tip is explained by more effective SIF when compared to critical SIF at that instance.

A similar characteristic crack behavior was noticed when the pressure of 4MPa was applied on the fracture geometry. Figure 4.20 shows the fracture geometry and wide crack opening.

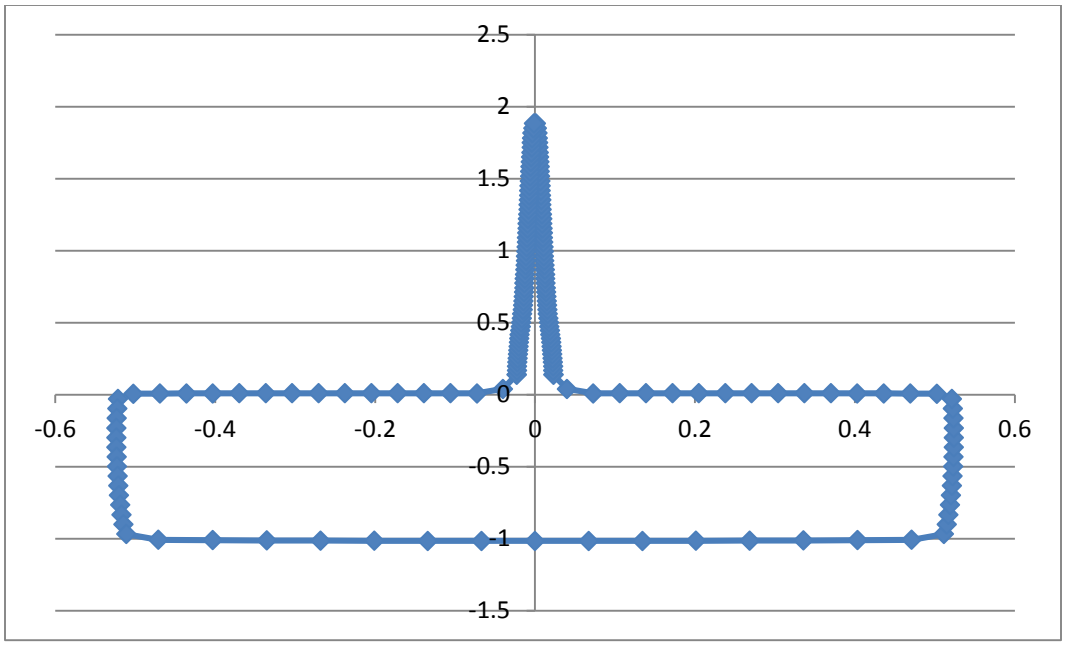

Figure 4.20 Fracture geometry when 4MPa pressure is applied

As projected, high pressure value causes the crack to propagate a much larger distance, which increases the distance between fluid front and the crack tip. This can be visualized from the figure 4.21a and 4.21b. As we go on increasing the pressure value, the effective stress intensity factor goes on increasing and hence the crack advances more distance so as to sustain the high pressure. The fluid front halts during this duration. But instead of the fluid front propagating ahead, the fluid pressure keeps on acting on the walls of the crack, creating a wider opening, thereby allowing more fluid to enter the crack.

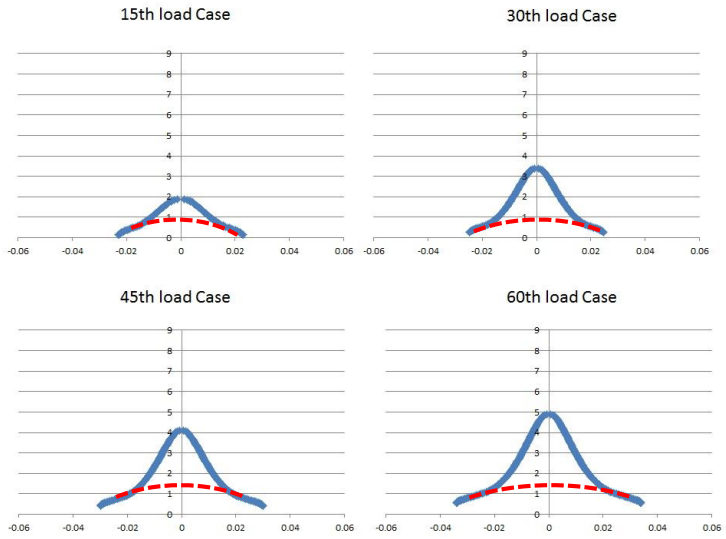

(a)

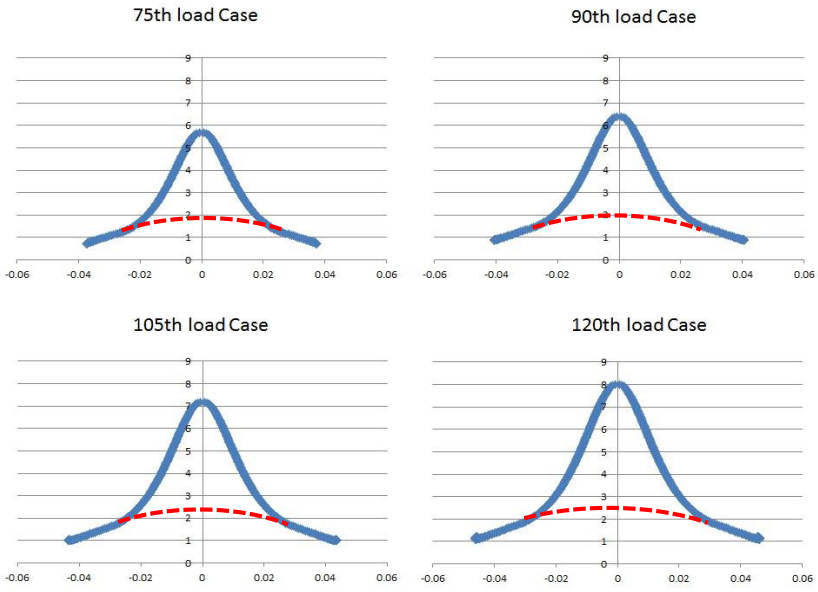

(b)

Figure 4.21 Crack propagating under pressure of 4 MPa (a) for 15th to 60th load case (b) for 75th to 120th load case

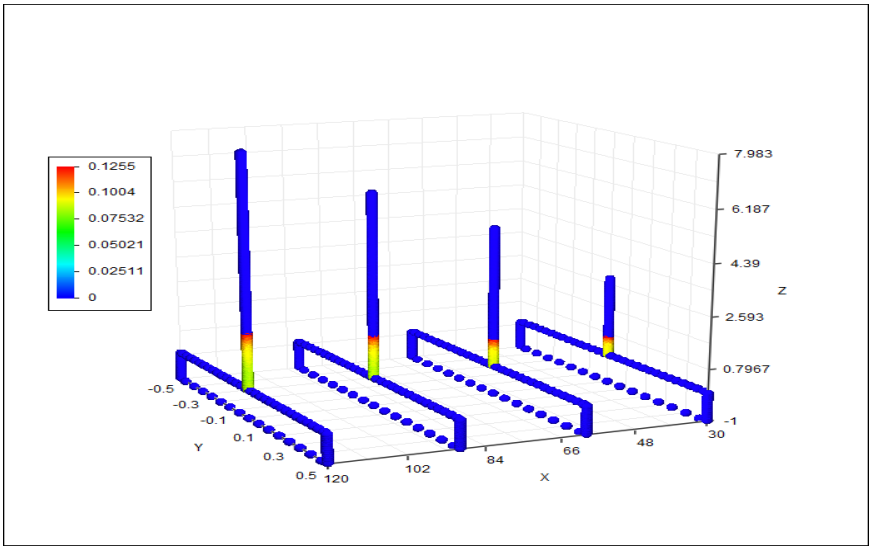

Figure 4.22 Velocity Profile of the fluid inside the fracture geometry

The color graph in the figure 4.22 shows till where the fluid front has reached. The velocity profile in the above graph proves that when the pressure increases the fluid lag also keeps on increasing.

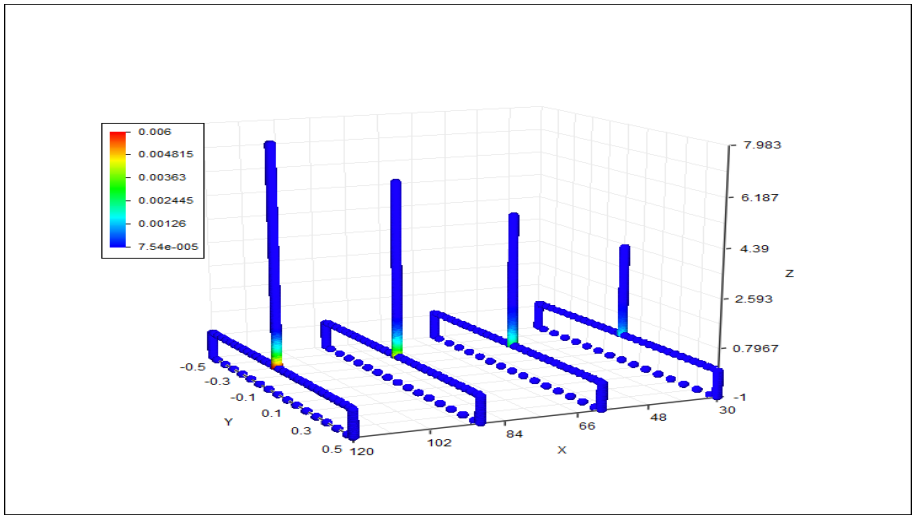

Figure 4.23 Crack Opening Profile of the fracture geometry

As the crack propagates and large fluid lag, the far field stresses keeps on acting on the crack from outside and tries to shut the crack. It is the pressure from the fluid, acting on the walls which overcomes these stresses and keeps the crack profile open. This phenomenon can be seen in the figure 4.23. Further the crack tip from the fluid tip, the opening of the crack is very small.

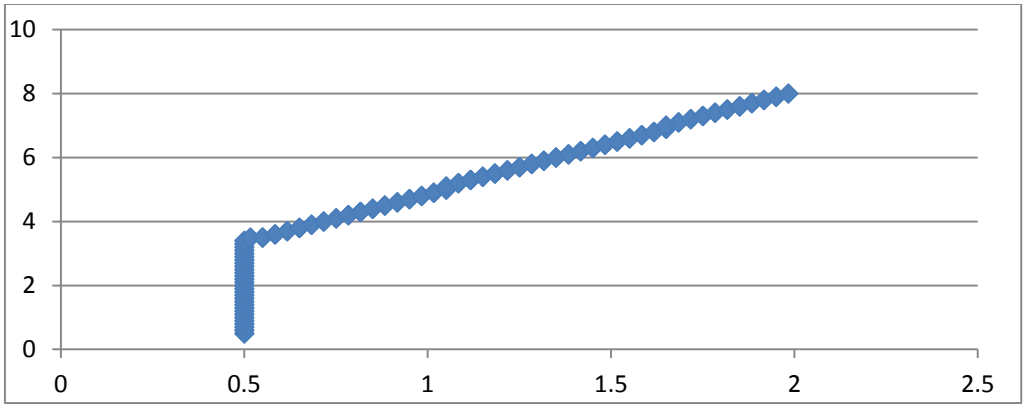

Figure 4.24 Graph of Fluid tip Vs. Crack tip

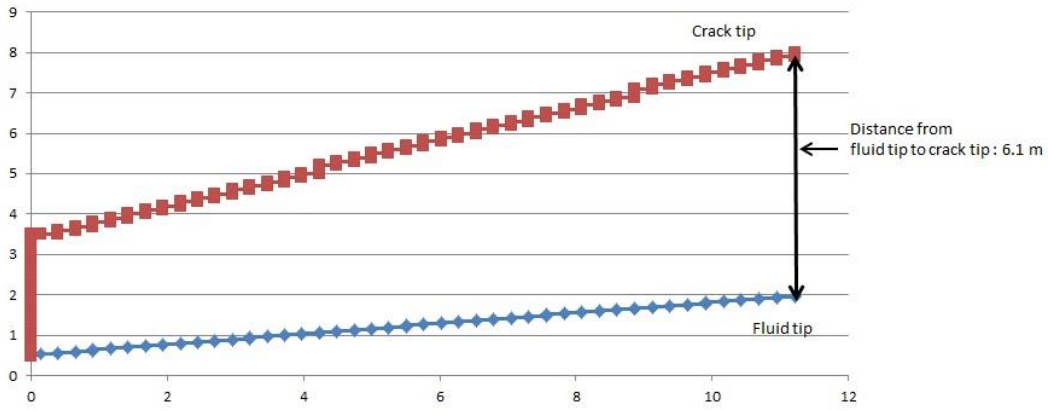

Figure 4.25 Graph showing distance between fluid tip and crack tip (fluid lag) when pressure of 4MPa is applied

Figure 4.24 and 4.25 support the statement that, higher the pressure value, higher is the fluid lag and it keeps on getting difficult to control the crack propagation.

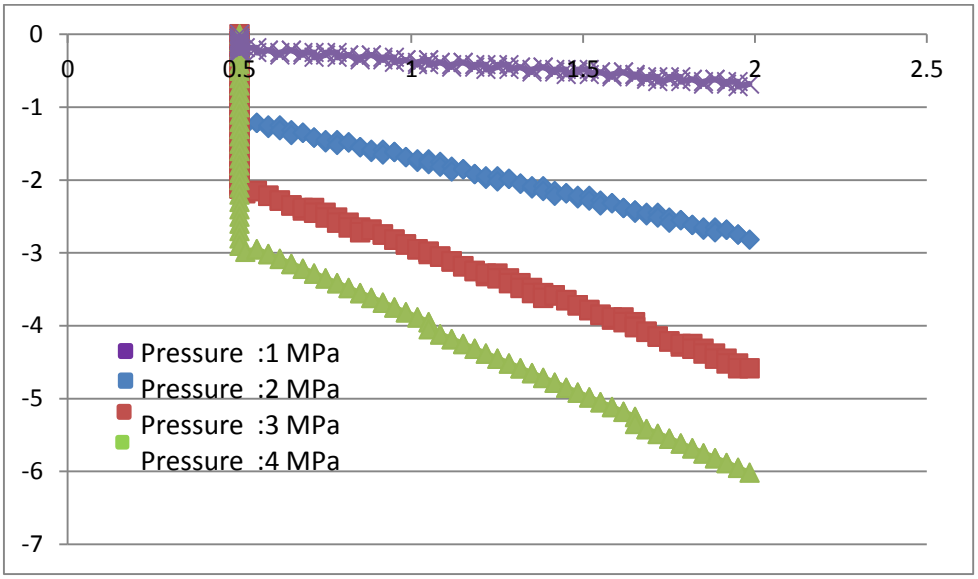

Figure 4.26 Graph showing fluid lag for different pressures Vs. Fluid tip

Figure 4.26 is the summation of all four cases showing the graph of fluid tip vs. fluid lag. If we ae to stand at the fluid tip and look at the crack tip propagating ahead of us, we would see that with every increase of fluid pressure the distance between us and the crack tip increases gradually. It can be concluded that to control the crack propagation, the fluid lag should not be large enough.

Above study was conducted on single crack propagation. The study is extended to crack branching and hydraulic fracture interaction with preexisting fracture. The results are showing some interesting crack behavior.

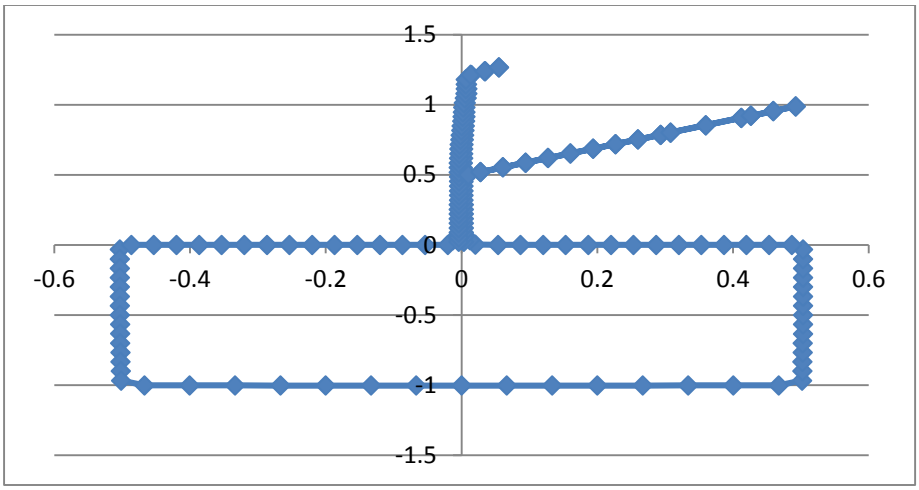

Figure 4.27 Crack branching geometry when 1 MPa pressure is applied

For the study of crack branching, rock elasticity was chosen to be 50Gpa and viscosity to be 500cp. Pressure of 1 MPa was applied in this case. Figure 4.27 shows the fracture geometry when the branched crack propagates under 1MPa pressure.

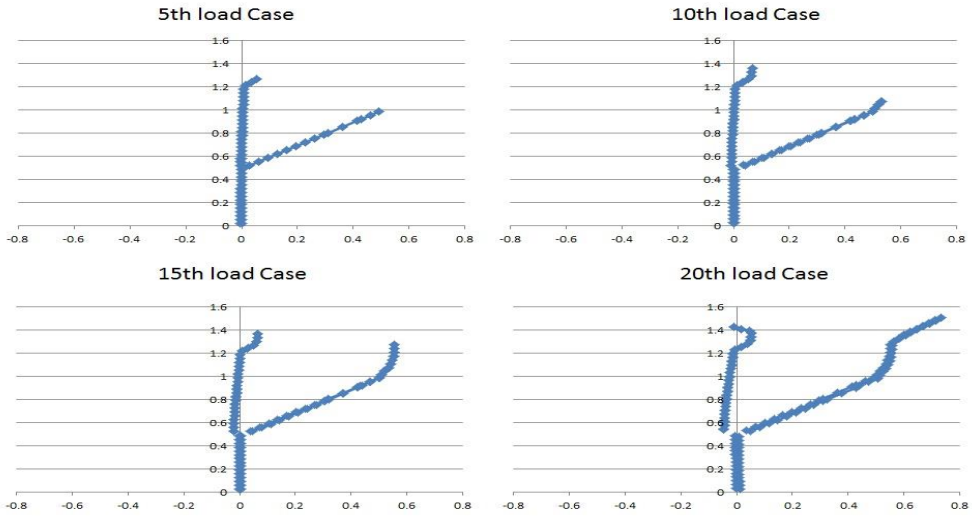

Figure 4.28 Crack propagating under pressure of 1 MPa

Initially as the fluid enters the crack, it simultaneously flows into the branched crack and towards the crack tip. As seen in figure 4.28, for the 5th load case, both cracks tend to propagate because of high stress region created at the crack tip. But as the branched crack propagates, its opening widens and hence it allows more fluid to flow through the crack. This gets the other crack tip arrested. More fluid flows through the branched crack and crack tip keeps on propagating till the pressure is not enough to make the crack propagate further. In other words, the effective stress intensity factor is high enough than critical SIF to make the crack advance further.

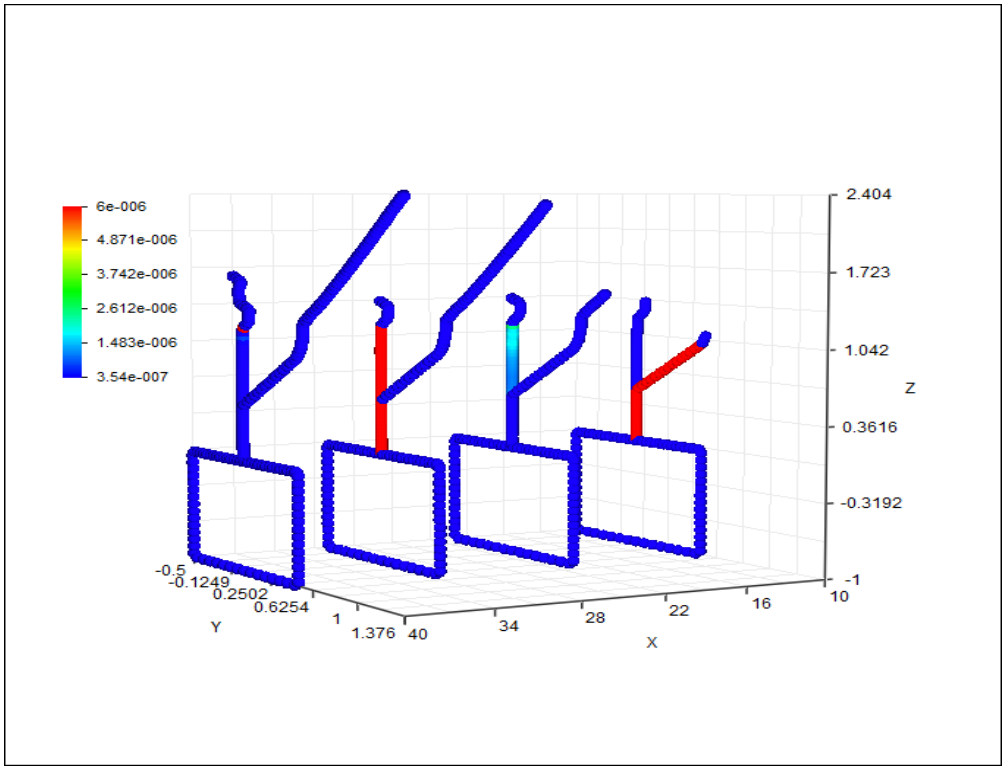

Figure 4.29 Velocity Profile of the fluid inside the fracture geometry

The velocity profile shown in figure 4.29 supports the phenomena. As seen in the first plot (first from right) the fluid flows through the branched crack and develops the crack profile. Stopping of the branched crack tip reactivates the other crack profile and fluid starts flowing in to the other crack as seen in the second plot(second from right). This crack then propagates till the pressure is not enough to develop the profile further. Once the crack stop propagating, the branched crack is activated again and fluid flowing through the crack overcomes the stresses, closing the crack, and further develops the crack profile.

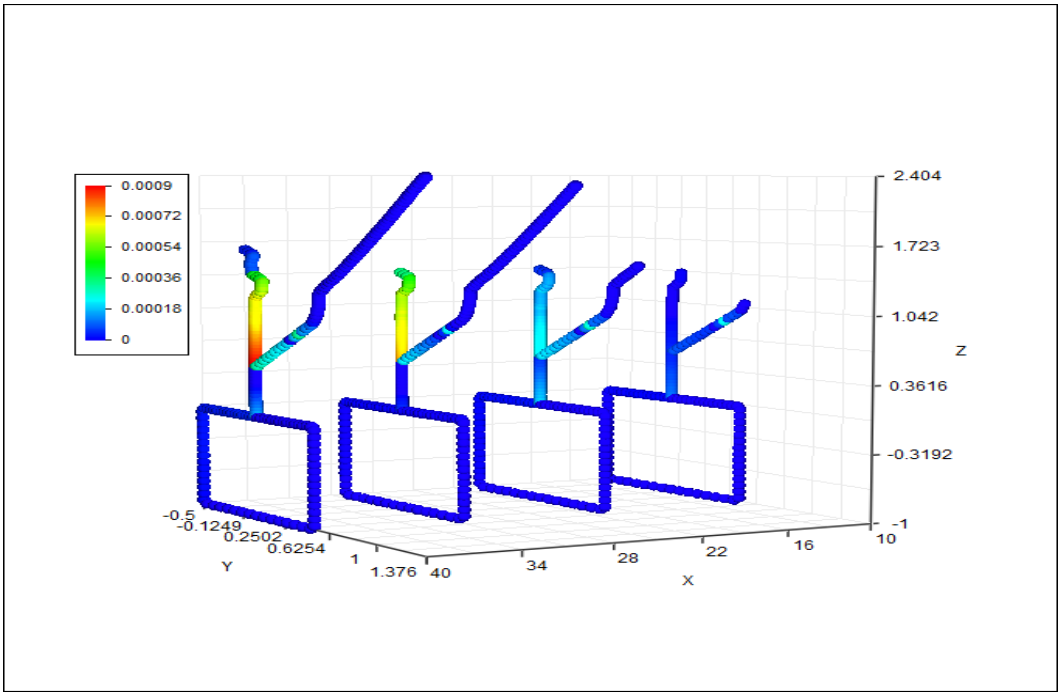

Figure 4.30 Crack Opening Profile of the fracture geometry

The opening profile of the branched network of crack is seen in figure 4.30. Interesting situation in observed in the third plot (third from right) as the

width of the crack at the entry point, near the wellbore, seems to be almost closed. That is because, as the branched crack was propagating, the walls of the fracture pushed aside the nearby rocks and hence more stress started acting in the walls at the entry point. The fluid pressure acting on the walls from within was not sufficient to keep the crack open and hence it almost shuts. This creates a wide opening at the branching junction as the fluid continuously tries to pressurize the walls of the crack in order to move ahead.

Another interesting study was carried out considering the fracture interacting with the preexisting crack. Two case studies were carried out, one considering longer preexisting crack and other having smaller preexisting crack.

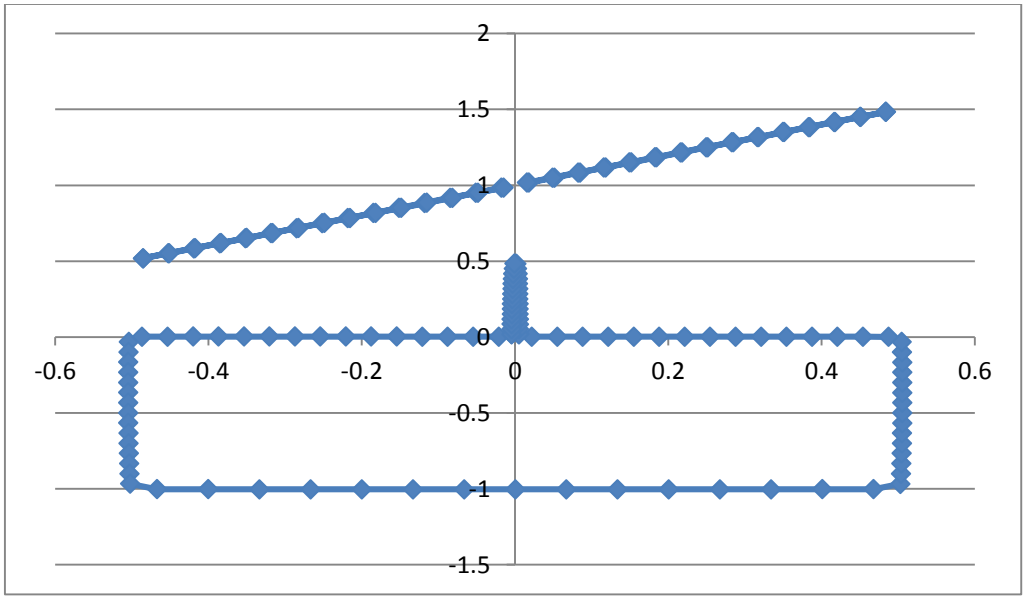

Figure 4.31 Hydraulic fracture and natural fracture geometry when 1 MPa pressure is applied.

Figure 4.31 shows the fracture geometry having a longer preexisting crack. The input parameters selected were rock elasticity 50GPa, Viscosity 500cp, Critical SIF of 1 Pa$\sqrt{m}$. Pressure of 1MPa was applied to study the characteristic behavior of the crack development.

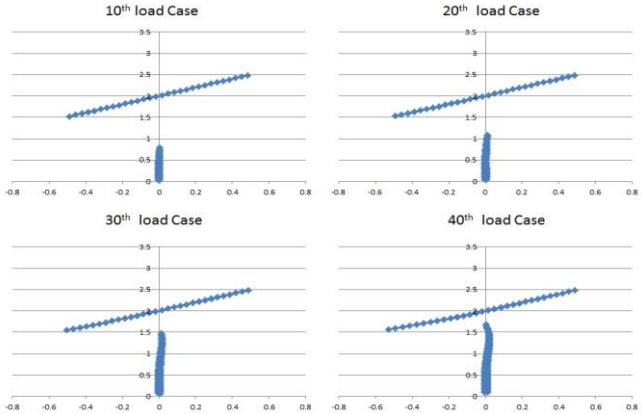

(a)

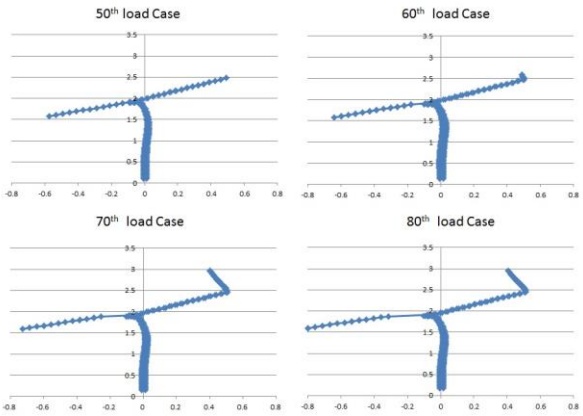

(b)

Figure 4.32 Crack propagating under pressure of 1 MPa (a) for 10th to 40th load case (b) for 50th to 80th load case

The crack profile develops as the fluid flows through it. As the crack approaches the preexisting crack, it tends to follow a wavy path and meets the crack perpendicular to the orientation of the preexisting crack as seen in the plots in the figure 4.32a. In figure 4.32b, we see a different crack behavior. Instead of intersecting the preexisting crack, the crack bends, shears through and pulls along the existing crack. An unusual behavior is noticed from load 60^{th} to 120^{th}. The existing crack seems to propagate without fluid flowing through it.

As the hydraulic fracture approaches the preexisting crack, it pushes aside the nearby rocks. This creates a high stress region at the crack tip of the existing crack, unbearable to sustain without breaking and hence the crack seems to propagate without hydraulic loading.

The velocity profile shown in figure 4.33 shows that as the fracture propagates, the fluid front follows with small fluid lag. As the fracture shears through the preexisting crack, fluid velocity keeps on building up as it can be seen the velocity plots with maximum at the crack tip.

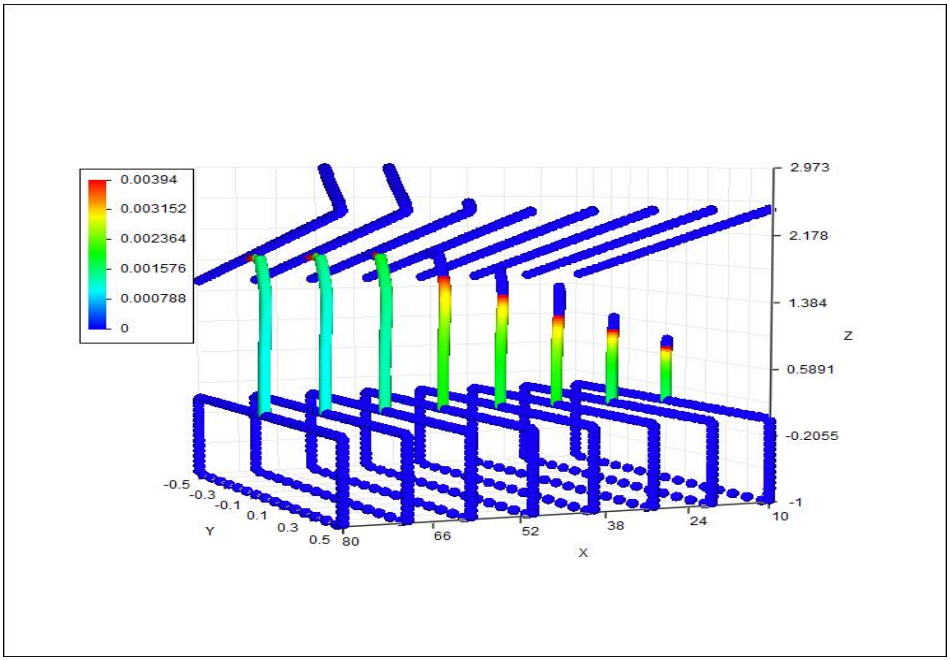

Figure 4.33 Velocity Profile of the fluid inside the fracture geometry

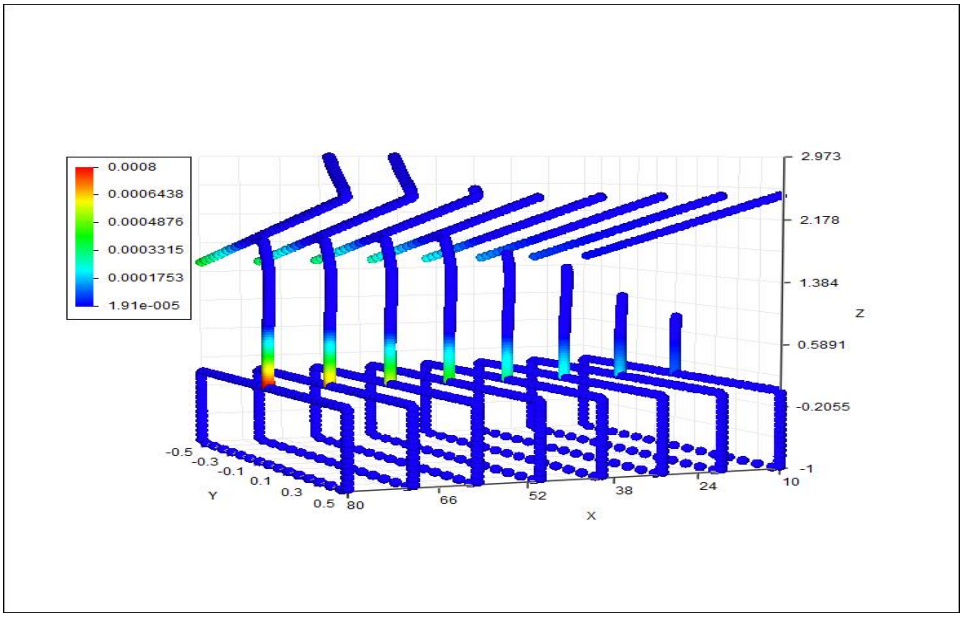

Figure 4.34 Crack Opening Profile of the fracture geometry

As the crack profile develops the fracture width keeps on increasing. Eventually as it approaches the preexisting crack, the shear force increases the aperture of the natural crack which can be seen in the opening profile plots shown in figure 4.34.

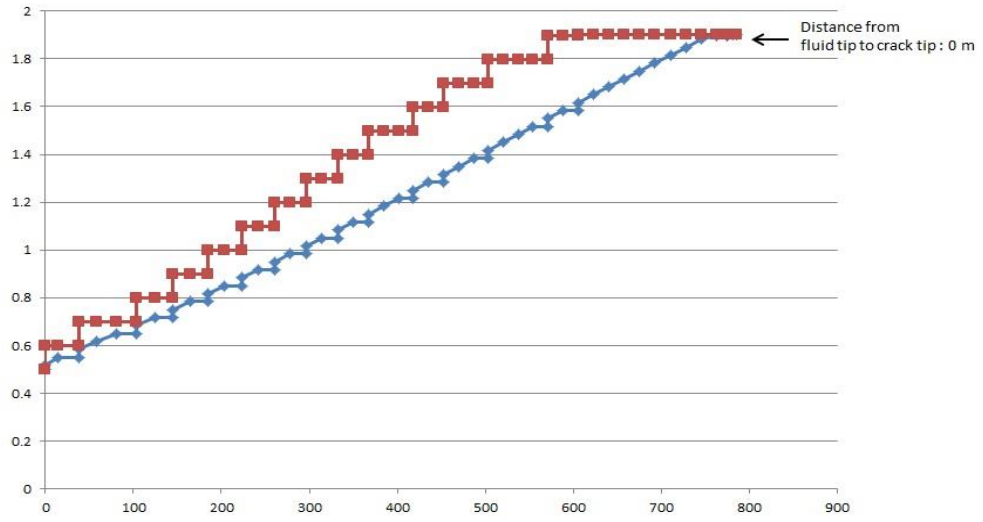

Figure 4.35 Graph showing distance between fluid tip and crack tip (fluid lag) when pressure of 1MPa is applied.

The evidence that the fluid does not enter the natural crack can be seen in figure 4.35. As seen earlier in the velocity plot, the geometry shows fluid lag, is proved from the above figure, but as the fracture interacts with the natural crack, the distance between the crack and fluid tip diminishes. High effective stress intensity factor does not allow the crack to develop further.

Following results show the characteristic crack behavior when it approaches smaller natural fracture.

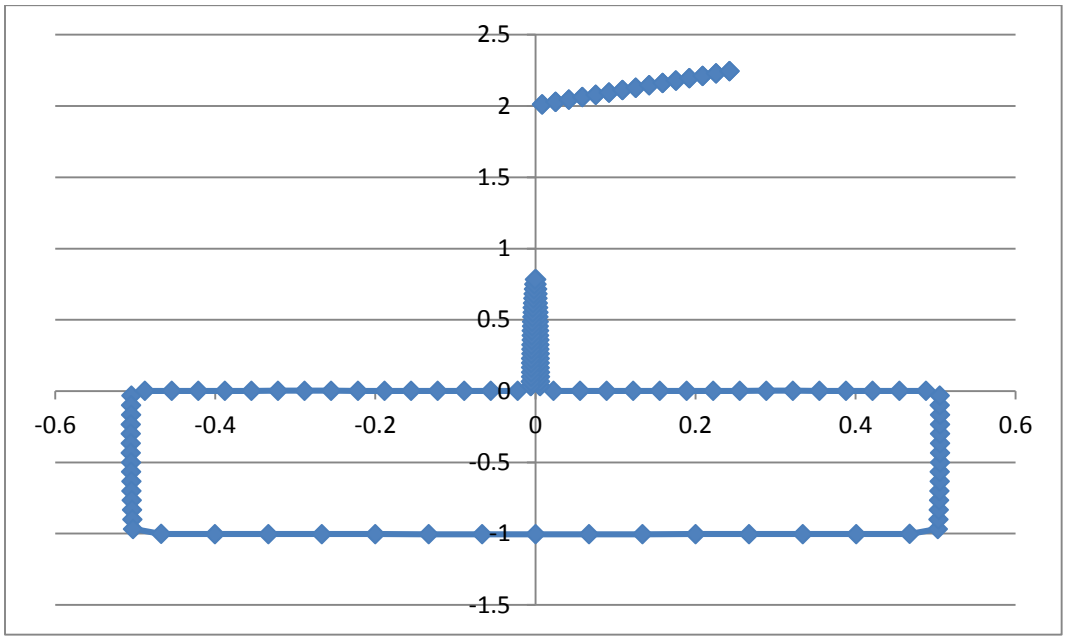

Figure 4.36 Hydraulic fracture and small natural fracture geometry when 1 MPa pressure is applied.

Same input parameters were applied as for the long natural fracture case to see if the hydraulic fracture still approaches the natural crack and interacts with it or bypasses it.

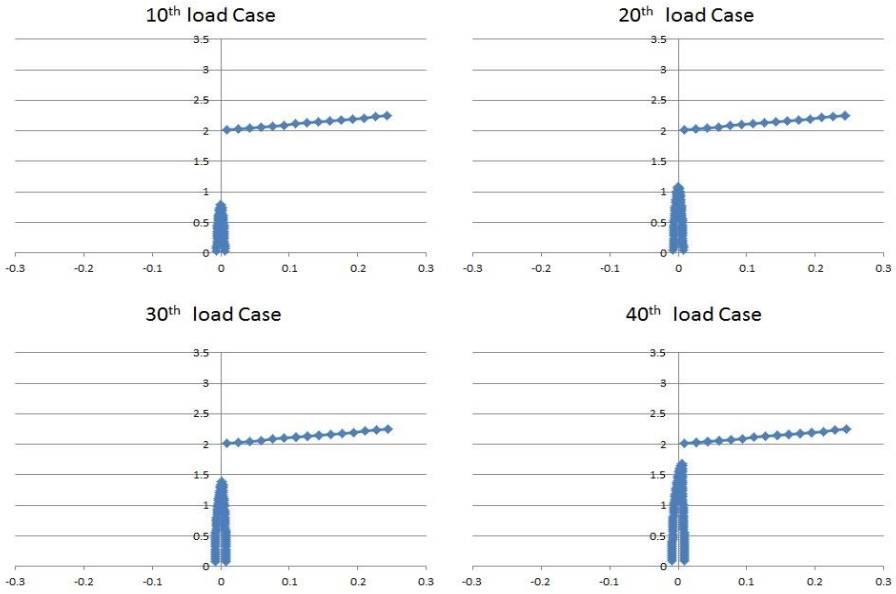

(a)

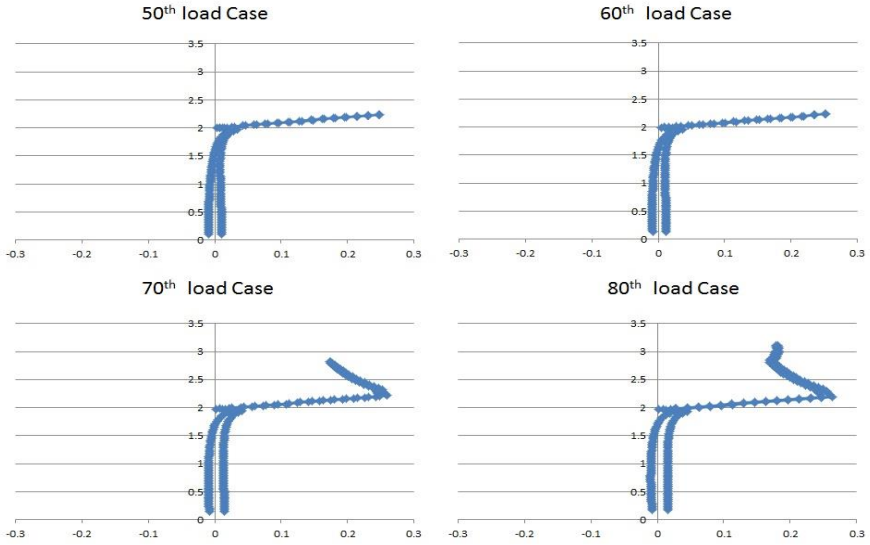

(b)

Figure 4.37 Fracture propagating and interacting with natural crack under pressure of 1 MPa (a) for 10^{th} to 40^{th} load case (b) for 50^{th} to 80^{th} load case

From figure 4.37a and 4.37b, it is proved that even for the smaller preexisting fracture; the hydraulic fracture approaches it and interacts with it. The hydraulic facture penetrates the natural crack, fluid enters the preexisting crack and fracture network starts developing. The fluid propagation can be seen in the velocity plots shown in figure 4.38.

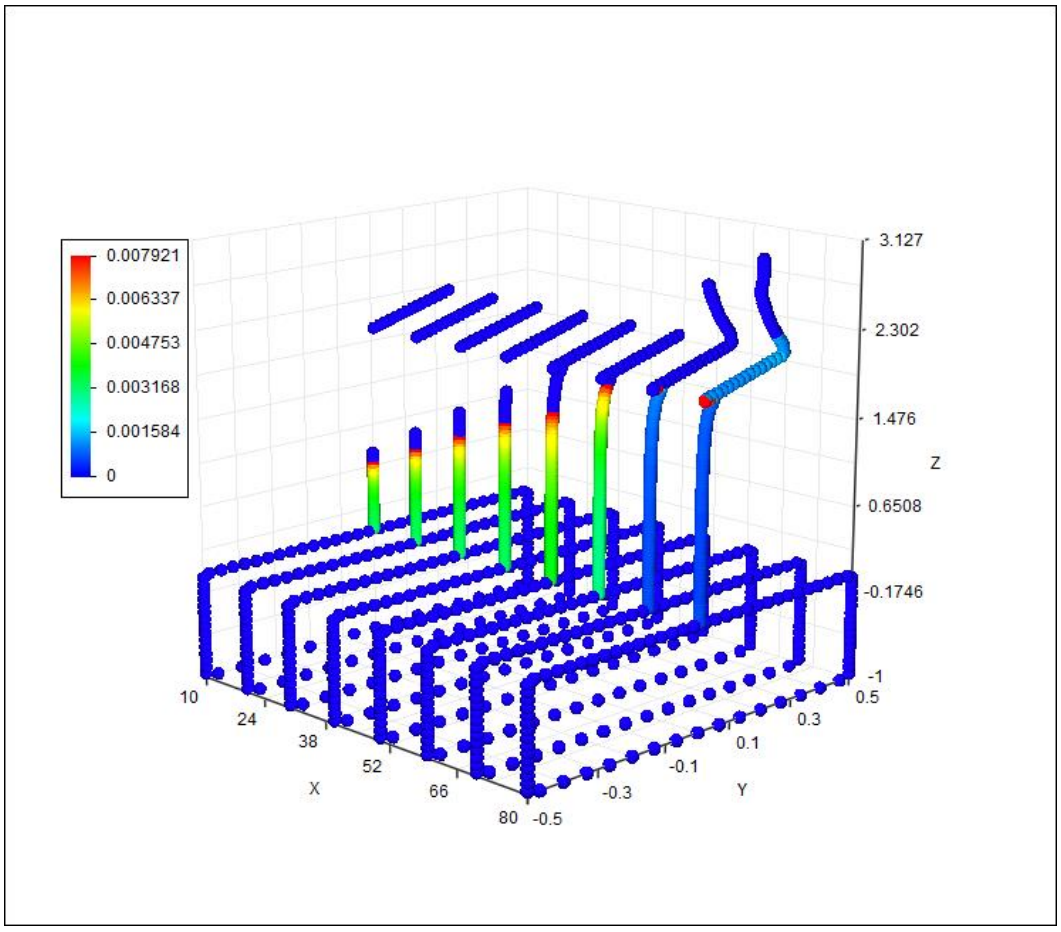

Figure 4.38 Velocity Profile of the fluid inside the fracture geometry

The fluid front follows the crack tip till it interacts with the natural crack. Once the crack penetrates the natural crack, the fluid enters the crack and starts developing the crack network.

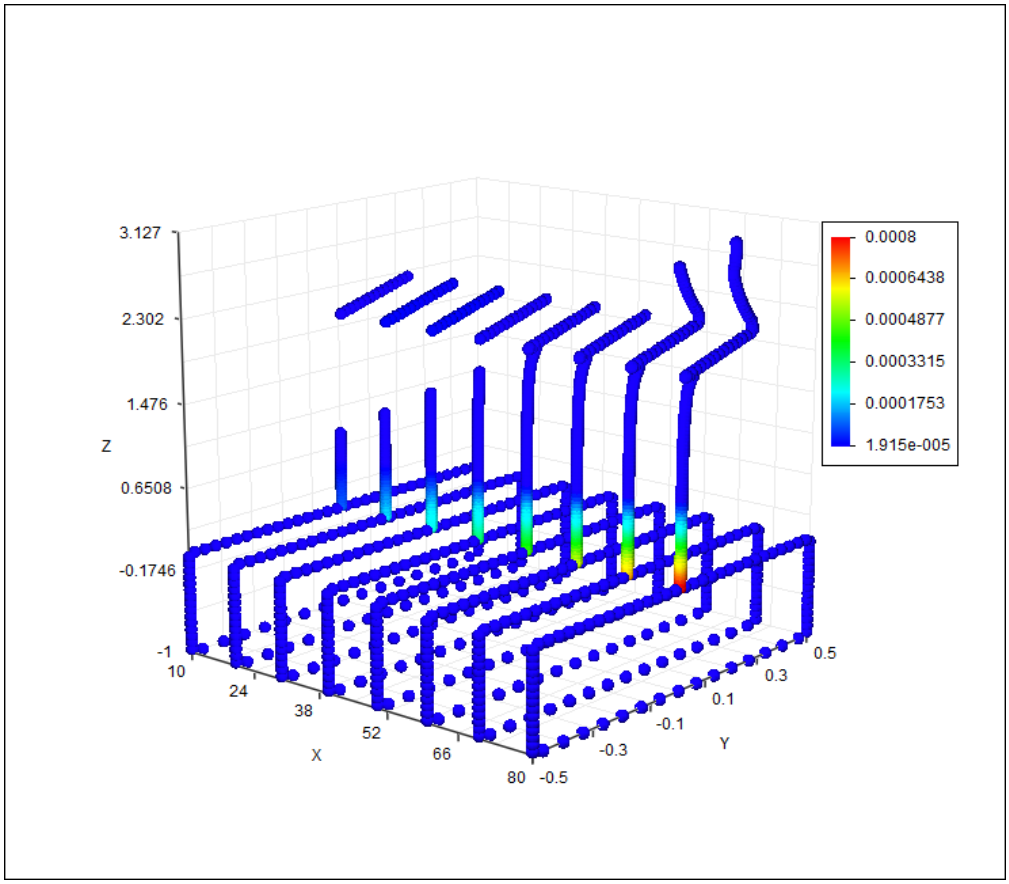

Figure 4.39 Crack opening profile of the fracture geometry

The fluid aperture gradually opens as the amount of fluid into the fracture increases. The blue region on the preexisting crack represents very small opening and hence very small fluid velocity as seen in the velocity plot.

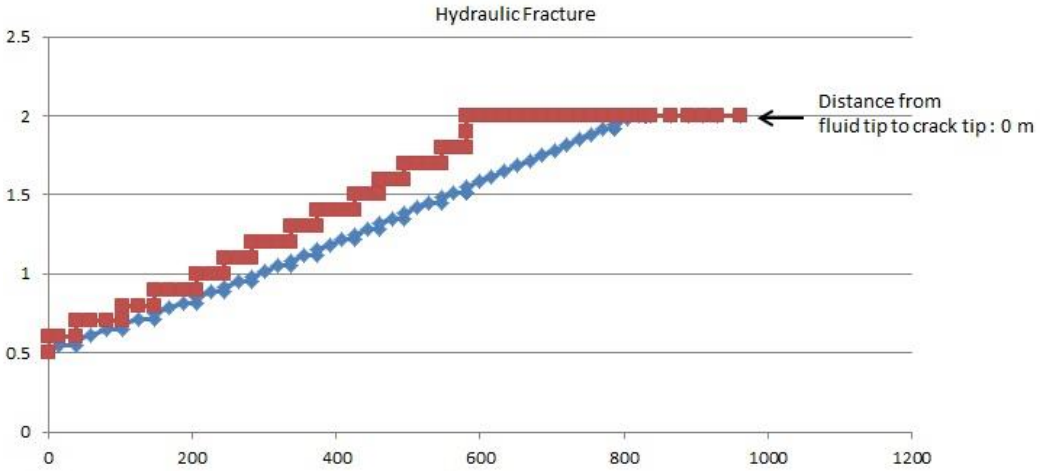

Figure 4.40 Graph showing distance between fluid tip and crack tip (fluid lag) when pressure of 1MPa is applied.

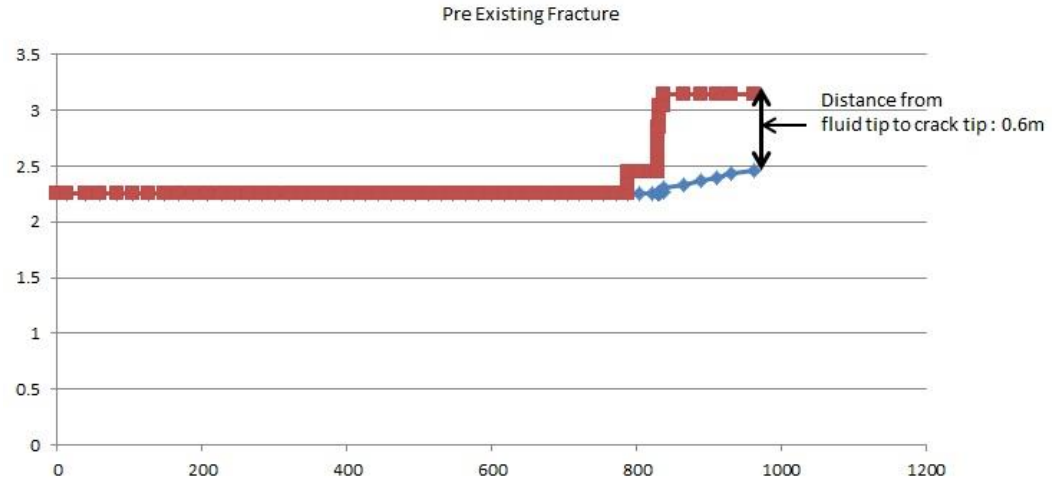

Figure 4.41 Fluid lag in preexisting crack when pressure of 1MPa is applied.

Figure 4.40 and 4.41 show the fluid lag during the fracture network development process. In figure 4.41 the graph starts developing only after hydraulic crack penetrates the natural crack.

Chapter 5

CONCLUSION

Fluid-crack interaction and network development was analyzed in this study. Linear Elastic Fracture Mechanics (LEFM) approach was used to understand the mechanical response of the hydraulic fracture. The Boundary element method (BEM) approach was used to calculate the results. Different cases were studied, starting with single crack geometry to gain complete understanding the fluid crack interaction phenomenon. The understanding was further applied to more complex geometry considering crack branching and hydraulic fracture interacting with natural crack. It can be concluded from the results that in order to gain control over crack propagation, having a good understanding of the fluid-crack interaction and material properties of the shale rock is necessary. Rock elasticity and viscosity play a key role in the amount of pressure required to maximize the fracture network. Increasing the pressure of the fracturing fluid may cause the propagation process to go out of control which may lead the fracture to penetrate the drinking water reserves, thereby posing a threat to pollute the reserve.

REFERENCES

[1] Adachi, J. I., and E. Detournay. "Self-similar solution of a plane-strain fracture driven by a power-law fluid." International Journal for Numerical and Analytical Methods in Geomechanics 26.6 (2002): 579-604.

[2] Carter, B. J., et al. "Simulating fully 3D hydraulic fracturing." Modeling in geomechanics 200 (2000): 525-557.

[3] Chaudhary, Anish Singh. Shale oil production performance from a stimulated reservoir volume. Diss. Texas A&M University, 2011.

[4] Chen, Zuorong. "An ABAQUS implementation of the XFEM for hydraulic fracture problems." Effective and Sustainable Hydraulic Fracturing (2013): 725-739.

[5] Chuprakov, Dimitry, Olga Melchaeva, and Romain Prioul. "Hydraulic fracture propagation across a weak discontinuity controlled by fluid injection." Effective and sustainable hydraulic fracturing, InTech (2013): 183-210.

[6] Cruse, THOMAS A., and W. Suwito. "On the Somigliana stress identity in elasticity." Computational Mechanics 11.1 (1993): 1-10.

[7] Fairhurst, Charles. "Fractures and fracturing: hydraulic fracturing in jointed rock." ISRM International Conference for Effective and Sustainable Hydraulic Fracturing. International Society for Rock Mechanics, 2013.

[8] Garagash, Dmitry I. "Propagation of a plane-strain hydraulic fracture with a fluid lag: Early-time solution." International journal of solids and structures 43.18 (2006): 5811-5835.

[9] Helms, Lynn. "Horizontal drilling." DMR newsletter 35.1 (2008): 1-3.

Klimczak, Christian, et al. "Cubic law with aperture-length correlation: implications for network scale fluid flow." Hydrogeology Journal 18.4 (2010): 851-862.

[10] Hubbert, M. King, and David G. Willis. "Mechanics of hydraulic fracturing." (1972): 239-257.

[10] Kear, James, et al. "Three dimensional forms of closely-spaced hydraulic fractures." Effective and Sustainable Hydraulic Fracturing (2013).

[12] Kresse, Olga, et al. "Effect of flow rate and viscosity on complex fracture development in UFM model." The International Conference for Ef-fective and Sustainable Hydraulic Fracturing. 2013.

[13] Kresse, Olga, and Xiaowei Weng. "Hydraulic Fracturing in Formations with Permeable Natural Fractures." ISRM International Conference for Effective and Sustainable Hydraulic Fracturing. International Society for Rock Mechanics, 2013.

[14] Linkov, Alexander M. "Solution of hydraulic fracture problem accounting for lag." arXiv preprint arXiv:1404.5246 (2014).

[15] Linsbauer, H. N. "Fluid-structure interaction related aspects during the grouting of cracks in concrete." ICF10, Honolulu (USA) 2001. 2013.

[16] Lo, Li Wei. Interaction of growing cracks in hydraulic fracturing. THE UNIVERSITY OF TEXAS AT ARLINGTON, 2014.

[17] Montgomery, Carl. "Fracturing fluids." Effective and Sustainable Hydraulic Fracturing (2013): 3-24.

[18] N. Weber, P. Siebert, K. Willbrand, M. Feinendegen, C. Clauser and T. P. Fries (2013). The XFEM with an Explicit-Implicit Crack Description for Hydraulic Fracture Problems, Effective and Sustainable Hydraulic Fracturing, Dr. Rob Jeffrey (Ed.), ISBN: 978-953-51-1137-5, InTech, DOI: 10.5772/56383.

[19] Riahi, Azadeh, and Branko Damjanac. "Numerical study of interaction between hydraulic fracture and discrete fracture network." submitted for publication in the Proceedings of International Conference for Effective and Sustainable Hydraulic Fracturing. 2013.

[20] Sarkar, Sudipta, M. Nafi Toksoz, and Daniel R. Burns. Fluid flow modeling in fractures. Massachusetts Institute of Technology. Earth Resources Laboratory, 2004.

[21] Sheibani, Farrokh, and Jon Olson. "Stress intensity factor determination for threedimensional crack using the displacement discontinuity method with applications to hydraulic fracture height growth and non-planar propagation

paths." The International Conference for Effective and Sustainable Hydraulic Fracturing, Brisbane, Australia. 2013.

[22] Spence, D. A., and P. Sharp. "Self-similar solutions for elastohydrodynamic cavity flow." Proceedings of the Royal Society of London. A. Mathematical and Physical Sciences 400.1819 (1985): 289-313.

[23] Yang, B., and K. Ravi-Chandar. "A single-domain dual-boundary-element formulation incorporating a cohesive zone model for elastostatic cracks." International Journal of Fracture 93.1-4 (1998): 115-144.

[24] Yang, B., and K. Ravi-Chandar. "Evaluation of elastic T-stress by the stress difference method." Engineering Fracture Mechanics 64.5 (1999): 589-605.

[25] Zhang, Xi, Robert G. Jeffrey, and Ella María Llanos. "On plane-strain fluid-driven shear fracture propagation in elastic solids." Geophysical Journal International 163.1 (2005): 419-430.

[26] Zimmerman, Robert W., and In-Wook Yeo. "Fluid Flow in Rock Fractures: From the Navier-Stokes Equations to the Cubic Law." Dynamics of fluids in fractured rock (2000): 213-224.

BIOGRAPHICAL INFORMATION

The author of this work obtained his undergraduate degree at University of Pune, India. His area of specialization was production engineering with emphasis in Computer Aided Design, Finite Element Analysis and Manufacturing Technology. After obtaining his bachelor degree, he worked for Analyzer-CAE solutions Pvt. Ltd., Pune as a FEA engineer from where he worked on contract with Cummins Research and Technology India, also as FEA engineer, responsible for modelling and analysis of generator components and sub components. Since August 2013, he has been working on his graduate program in Mechanical Engineering at the University of Texas at Arlington. His areas of interest include Finite Element Methods, Fracture Mechanics, and Fluid Mechanics.